

# Ablation of Cavotricuspid Isthmus–Dependent Atrial Flutters

*Gregory Feld, David Krummen, Jonathan Hsu, Kurt Hoffmayer, Farah Z. Dawood, Gordon Ho*

## KEY POINTS

- The mechanism of most cavotricuspid isthmus (CTI)-dependent atrial flutter (AFL) is macroreentry around the tricuspid valve annulus (TVA).
- The diagnosis of CTI-dependent atrial flutter is made by demonstration of macroreentry around the TVA during entrainment at two or more sites around the tricuspid valve, and demonstration of concealed entrainment from the CTI during AFL.
- The target for ablation of CTI-dependent AFL is the CTI, between the TVA and the inferior vena cava (IVC).
- Special equipment that may improve outcome or may be required to ablate the CTI includes a large-tip catheter (8- or 10-mm

- ablation electrode) with a high-power radiofrequency generator (up to 100 watts) or an externally irrigated ablation catheter, a large-curve catheter, and a preformed or steerable sheath. An intracardiac echocardiographic (ICE) catheter, electroanatomic or noncontact 3-dimensional mapping systems, or a multielectrode Halo catheter may be useful but are not required.
- Sources of difficulty in assuring successful long-term success may include complex anatomy (e.g., pouches, prominent Eustachian ridge) of the CTI, leading to failure to achieve bidirectional isthmus conduction block.
- Long-term success rates range from 90% to 95%, after achieving acute bidirectional CTI conduction block.

Cavotricuspid isthmus (CTI)-dependent atrial flutter (AFL) is a common atrial arrhythmia, often occurring in association with atrial fibrillation. It can cause significant symptoms because of a typically rapid ventricular rate, and may cause embolic stroke, and rarely a tachycardia-induced cardiomyopathy. The electrophysiologic substrate underlying CTI-dependent AFL has been shown to be macroreentry around the tricuspid valve annulus (TVA), with an area of concealed conduction in the CTI, anatomically bounded by the TVA anteriorly and the inferior vena cava (IVC) and Eustachian ridge posteriorly, with a line of conduction block along the crista terminalis. This electrophysiologic milieu produces a long enough reentrant path length, relative to the average tissue wavelength around the TVA, to allow for sustained reentry. The triggers of AFL, commonly premature atrial contractions or nonsustained atrial fibrillation originating from the left atrium and pulmonary veins, most likely account for the fact that counterclockwise AFL (typical AFL) occurs most frequently clinically. AFL is also relatively resistant to pharmacologic suppression.

Because of the consistent and well-defined anatomic substrate and the typical pharmacologic resistance of CTI-dependent AFL, radiofrequency (RF) catheter ablation is established as a safe and effective first-line treatment. Although several approaches have been described for ablating CTI dependent AFL, the most widely accepted technique is an anatomically-guided approach targeting the entire CTI, resulting in a high efficacy rate for cure of AFL, with minimal risk. This chapter reviews the electrophysiology of human CTI-dependent AFL and techniques currently used for its diagnosis, mapping, and ablation.

## ATRIAL FLUTTER TERMINOLOGY

Because of the variety of terms used to describe AFL in humans in the past, including type 1 and type 2 AFL, typical and atypical AFL,

counterclockwise (CCW) and clockwise (CW) AFL, and isthmus-dependent and non-isthmus-dependent AFL, the Working Group of Arrhythmias of the European Society of Cardiology and the North American Society of Pacing and Electrophysiology published a consensus document in 2001 in an attempt to develop a generally accepted standardized terminology for AFL.<sup>1</sup> The consensus was that the terminology “typical” and “type 1” AFL were most commonly used to describe CTI-dependent, defined as a macroreentrant right atrial tachycardia, and included both the CCW and CW variants rotating around the TVA. Therefore the working group determined that CTI-dependent, right atrial macroreentrant tachycardia, rotating in the CCW direction around the TVA (when viewed from the right ventricle) would be termed typical AFL, and the similar tachycardia rotating in the CW direction around the TVA would be termed reverse typical AFL.<sup>1</sup> For the purposes of this book, we will use the terms typical and reverse typical AFL, or CTI-dependent AFL when being referred to jointly. Other rare isthmus-dependent AFL variants, including lower loop reentry and partial isthmus-dependent AFL, are also discussed in this chapter.

## ANATOMY AND PATHOPHYSIOLOGY

The development of successful RF catheter ablation (RFCA) techniques for CTI-dependent AFL depended in part on the delineation of its electrophysiologic mechanism. Using advanced electrophysiologic techniques, including intraoperative and trans catheter activation mapping,<sup>2–7</sup> CTI-dependent AFL was shown to be caused by a macroreentrant circuit rotating in either a CCW (typical) or a CW (reverse typical) direction in the right atrium around the TVA, with an area of relatively slow conduction velocity in the low posterior right atrium (*Figs. 11.1 and 11.2*). The predominant area of slow conduction in the AFL reentry circuit has been

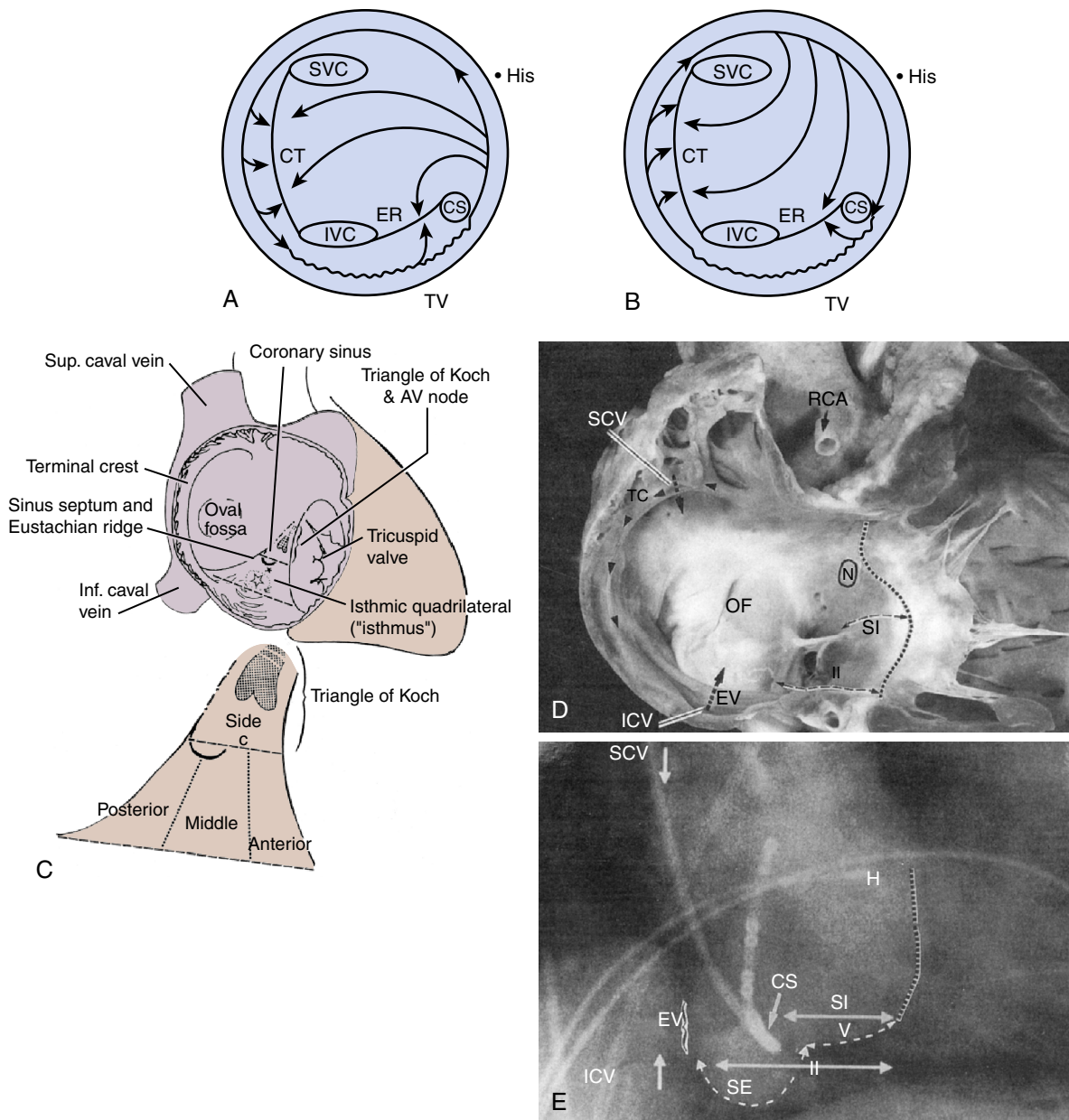


**Fig. 11.1** A and B, Schematic diagrams showing the activation patterns of CTI-dependent AFL, as viewed from below the tricuspid valve (TV) annulus, looking up into the right atrium. In typical AFL (A), the reentrant wave front rotates counterclockwise in the right atrium (RA), but in reverse typical AFL (B), reentry is clockwise. Note that the Eustachian ridge (ER) and crista terminalis (CT) form lines of block and that an area of slow conduction (wavy line) is present in the CTI (between the ER and TV annulus). CS, Coronary sinus ostium; His, His bundle; SVC, superior vena cava. C–E, Anatomy of the CTI. The schematic diagram of the right atrium (C) shows the CTI (expanded insert), which is posterior and inferior to the triangle of Koch. D, Pathologic specimen showing the heart in right anterior oblique (RAO) view. The hinge of the TV is shown by the dotted line. Note the complex anatomy along the inferior isthmus line, with a fenestrated Thebesian valve present. SI, Septal isthmus; II, inferior isthmus; EV, Eustachian valve; OF, foramen ovale; N, AV nodal area; SVC, superior vena cava. E, RAO angiogram of the CTI. A pouch-like sub-Eustachian sinus (SE) is seen adjacent to the vestibule region of the isthmus (V). H, His catheter. (From Cabrera JA, Sanchez-Quintana D, Ho SY, et al. The architecture of the atrial musculature between the orifice of the inferior caval vein and the tricuspid valve: the anatomy of the isthmus. *J Cardiovasc Electrophysiol*. 1998;9:1186-1195. With permission.)

shown to be in the CTI, through which conduction times may reach 80 to 100 ms, accounting for one-third to one-half of the AFL cycle length.<sup>8–10</sup>

The CTI is the target for ablation and warrants special attention. The CTI refers to right atrial myocardium between the TVA and IVC, which courses from the inferolateral to the posteromedial low right

atrium and is anatomically bounded by the IVC and Eustachian ridge posteriorly and by the TVA anteriorly (see Figs. 11.1 and 11.2). These boundaries form lines of conduction block delineating a protected zone in the reentry circuit.<sup>11–14</sup> The presence of conduction block along the Eustachian ridge<sup>11–14</sup> has been confirmed by the demonstration of

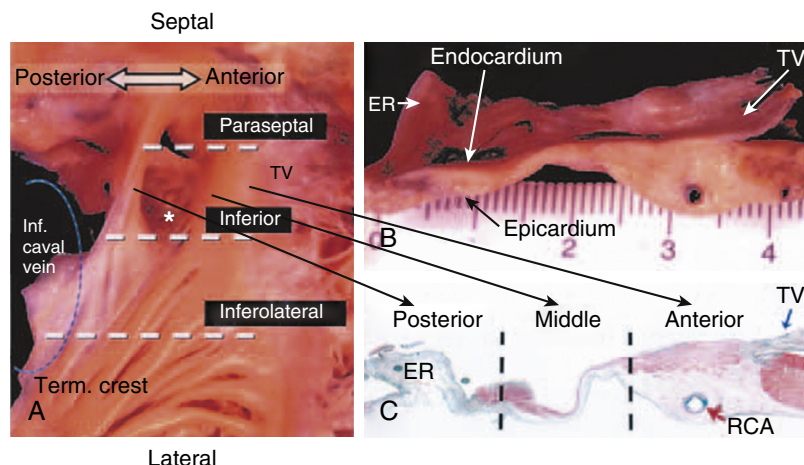


**Fig. 11.2** A, The endocardial surface of the right atrial cavotricuspid isthmus (CTI) is displayed to show the three levels. Note the pouch at the central isthmus and the distal ramifications of the terminal (Term.) crest that feed into the inferolateral CTI. B and C, The CTI viewed in profile. The histologic section shows myocardium in red and fibrous tissue in blue. The anterior sector corresponds to the vestibule leading to the tricuspid valve (TV) and is related to the right coronary artery (RCA). The posterior sector is closest to the orifice of the inferior caval vein and contains the Eustachian valve or ridge (ER) (Masson trichrome stain). (From Cabrera JA. The inferior right atrial isthmus: further architectural insights for current and coming ablation technologies. *J Cardiovasc Electrophysiol*. 2005;16:402-408. With permission.)

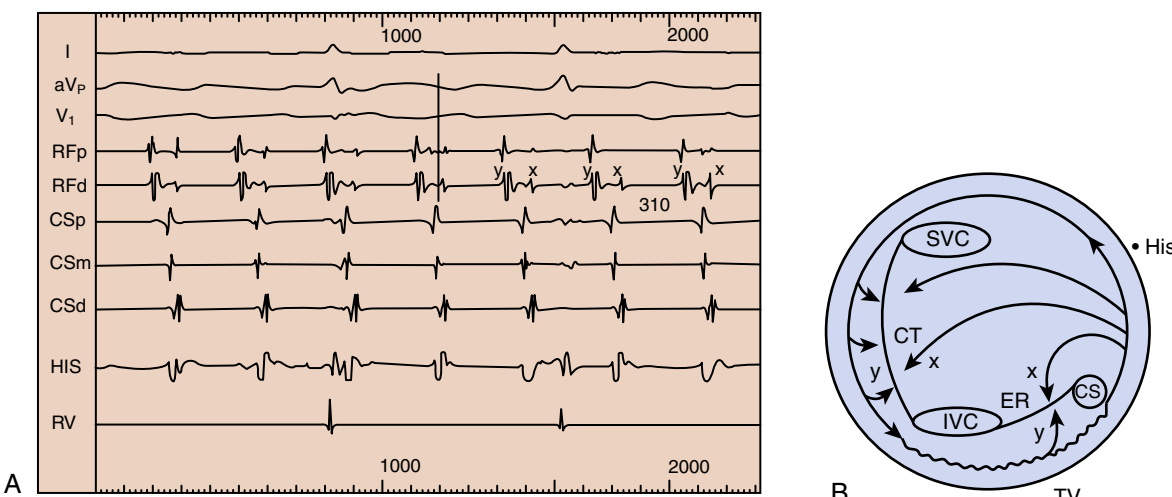


**Fig. 11.3** A, Surface electrocardiographic leads I, aVF, and V<sub>1</sub> and endocardial electrograms (EGMs) in a patient with typical atrial flutter (AFL) demonstrating double potentials (x,y) recorded along the Eustachian ridge (ER) by the ablation catheter (RFd and RFp). Note that the x and y potentials straddle the onset of the initial downstroke of the F wave in lead aVF (vertical line), indicating that the x potential is recorded immediately after the activation wave front exits the sub-Eustachian isthmus and circulates around the coronary sinus above the ER. The y potential is recorded after the activation wave front has rotated entirely around the atrium and is proceeding through the sub-Eustachian isthmus below the ER. Double potentials may similarly be recorded along the crista terminalis (CT). B, A schematic diagram of the right atrium indicates where double potentials (x,y) may be recorded along the ER and CT during typical AFL. CSp, CSm, and CSd are electrograms recorded, respectively, from the proximal, middle, and distal electrode pairs on a quadripolar catheter in the coronary sinus (CS) with the proximal pair at the ostium. His, Electrogram from the His bundle catheter; IVC, inferior vena cava; RFp and RFd, electrograms from the proximal and distal electrode pairs of the mapping and ablation catheter with the distal pair positioned on the ER; RV, right ventricle electrogram; SVC, superior vena cava; TV, tricuspid valve.

double potentials along its length during AFL (Fig. 11.3). The superomedial boundary of the CTI is the line between the septal insertion of the Eustachian ridge and the most inferior para-septal insertion of the tricuspid valve (TV) (i.e., the base of the triangle of Koch).<sup>15,16</sup> The inferolateral border of the CTI comprises the final ramifications of the

pectinate muscles of the crista terminalis, but a precise lateral boundary is not well defined. In attitudinal orientation, the portion of the CTI adjacent to the tricuspid annulus is anterior and sometimes referred to as the vestibular portion of the CTI. The portion of the CTI that is adjacent to the IVC is attitudinally posterior and referred to as the

membranous CTI. The middle portion of the CTI is referred to as the trabeculated CTI.<sup>15</sup>

The anatomy of the CTI can be assessed by computed tomography (CT) or magnetic resonance imaging (MRI) before ablation or by angiography, electroanatomic mapping, or echocardiography intraoperatively.<sup>17–19</sup> The CTI is typically  $34 \pm 5$  mm in length when measured angiographically from the IVC to the TV. The CTI is usually subdivided into three sections: septal isthmus, central isthmus, and lateral isthmus (see Figs. 11.1 and 11.2).<sup>15,19</sup> In the electrophysiology laboratory, the septal isthmus is defined as that portion between 4 and 5 o'clock when visualized in the left anterior oblique (LAO) projection fluoroscopically. The central isthmus is that portion located at 6 o'clock, and the lateral isthmus is that starting at 7 o'clock.<sup>15</sup> The central isthmus (6 o'clock) marks the shortest distance between the IVC and tricuspid annulus ( $19 \pm 4$  mm, range 13–26 mm).<sup>15</sup> In addition, the central isthmus is the thinnest portion, ranging from an average of 3.5 mm near the TV to 0.8 mm in the middle portion.<sup>15</sup> The anterior (vestibular) portion of the CTI adjacent to the TV is entirely muscular, whereas the posterior (membranous) portion closest to the IVC is primarily fibro-fatty tissue.<sup>15</sup> The muscle thickness is least in the central isthmus, greatest at the septal isthmus, and intermediate in the lateral isthmus.<sup>15</sup>

The anatomy of the CTI is highly variable but usually classified into three categories. A flat CTI shows 2 mm or less inferior concavity between the IVC and TV and is found in about 28% of patients.<sup>18,19</sup> A concave CTI with inferior concavity more than 2 mm in depth is found in about 20% of patients. In these, the average depth is  $3.7 \pm 0.8$  mm.<sup>19</sup> In up to 83% of patients, the CTI shows a distinct inferior pouch (sub-Eustachian pouch or sinus of Keith) averaging  $6.5 \pm 2.2$  mm in depth but up to 12.4 mm deep (see Figs. 11.1 and 11.2).<sup>15–19</sup> The pouch is separated from the TV by a smooth vestibular area (see Figs. 11.1 and 11.2).<sup>19</sup> The pouch itself may be symmetrical or asymmetrical, with extension toward the atrial septum. In anatomic studies, pouches are confined to the medial or septal CTI but are not seen in the lateral third of the CTI.<sup>20</sup> Other notable anatomic features influencing the success of CTI ablation are the presence of a prominent muscular Eustachian ridge in about 26% of patients, extension of pectinate muscles into the CTI in 70% of patients, and even into the coronary sinus in 7%.<sup>20</sup> The thickness of the pectinate muscles is greatest laterally and diminishes toward the atrial septum. The presence of pectinate muscles in the CTI may be suggested by recording high voltage electrograms (EGMs) from this area.<sup>20</sup> In autopsy specimens, CTI pectinate muscle extensions and CTI pouches tend to occur together.<sup>20</sup>

The crista terminalis forms another important boundary for CTI-dependent AFL. The crista terminalis leaves the superior right atrial septum and courses superiorly and anteriorly to the superior vena cava, and inferiorly along the posterolateral right atrial free wall to the IVC, where it then continues anteriorly and medially to form the Eustachian ridge. Double potentials have also been recorded along the crista terminalis,<sup>11–14</sup> suggesting that it too forms a line of block during AFL, separating the smooth septal right atrium from the trabeculated right atrial free wall (see Fig. 11.3). Such lines of block, which may be either functional or anatomic, are necessary for an adequate path length for reentry to be sustained, to prevent “short-circuiting” of the reentrant wave front.<sup>12–14,21</sup> Thus during typical AFL, the activation wave front traverses the CTI and exits medially, ascends the atrial septum, courses over the anterior right atrium, descends the right atrial lateral wall between the crista terminalis posteriorly and the TV anteriorly, and then enters the CTI laterally to complete the circuit.<sup>12–14,21</sup>

The medial and lateral CTI, which are contiguous, respectively, with the interatrial septum near the coronary sinus (CS) ostium and with the low lateral right atrium near the IVC (see Figs. 11.1 and 11.2),

correspond to the exit and entrance to the CTI, depending on whether the direction of reentry is CCW or CW in the right atrium.<sup>2–15</sup> The presence of slow conduction in the CTI, relative to the interatrial septum and right atrial free wall, may be caused in part by the anisotropic fiber orientation in the CTI.<sup>7–10,22,23</sup> This may also predispose to the development of unidirectional block during rapid atrial pacing, accounting for the observation that typical (CCW) AFL is more likely to be induced when pacing is performed from the CS ostium, and reverse typical (CW) AFL when pacing is from the low lateral right atrium.<sup>24</sup>

Lower-loop reentry is an isthmus-dependent flutter in which the caudal-to-cranial limb of the wave front crosses over gaps in the crista terminalis in the inferior to middle right atrium (Fig. 11.4).<sup>25,26</sup> The circuit is essentially around the ostium of the IVC in the right atrium. The direction of rotation may be CW or CCW. This variant activation sequence may be sustained, or it may interconvert with other forms of AFL.

Partial isthmus flutter is another variant in which the CCW reentrant wave front “short circuits” through the Eustachian ridge barrier to pass between the IVC and the CS ostium (see Fig. 11.4).<sup>25</sup> The wave front then propagates in a CW direction through the medial end of the CTI to collide with the wave front that is also conducting through the isthmus from its lateral aspect.

Intra-isthmus reentry (IIR) is a microreentrant atrial flutter localized within the septal region of the CTI (Fig. 11.5). In a prospective series of patients with IIR reported by the Yang, et al.,<sup>27,28</sup> around half of patients (57%) with intraisthmus had prior CTI ablation. IIR was often diagnosed in patients (21%) with recurrent atrial flutter after previous CTI ablation.

## DIAGNOSIS

### Surface Electrocardiography

The surface 12-lead electrocardiogram (ECG) is helpful in establishing a diagnosis of CTI-dependent AFL, particularly the typical form (Table 11.1). In typical AFL, an inverted saw tooth F wave pattern is observed in the inferior ECG leads II, III, and aVF, with low-amplitude biphasic F waves in leads I and aVL, an upright F wave in precordial lead V<sub>1</sub>, and an inverted F wave in lead V<sub>6</sub> (Fig. 11.6 A). In contrast, in reverse typical AFL, the F wave pattern on the 12-lead ECG is less specific and variable, often with a sine wave pattern in the inferior ECG leads (see Fig. 11.6 B). The determinants of F-wave pattern on ECG are largely dependent on the activation sequence of the left atrium, resulting from reentry in the right atrium. Inverted F waves are inscribed in the inferior ECG leads in typical AFL, because of activation of the left atrium initially posteriorly near the CS, and upright F waves are inscribed in the inferior ECG leads in reverse typical AFL because of activation of the left atrium initially anteriorly, near Bachmann's bundle.<sup>29,30</sup> However, because the typical and reverse typical forms of CTI-dependent AFL use the same reentry circuit, but in opposite directions, their rates are often similar. It has also been shown that the ECG presentation of typical AFL can be dramatically altered by ablation in the left atrium for atrial fibrillation.<sup>31</sup>

The ECG presentation of lower-loop reentry is highly variable, depending on the caudal-to-cranial level of wave front breakthrough across the crista terminalis.<sup>26</sup> CCW lower-loop reentry may resemble typical AFL because of similar patterns of activation of the atrial septum and left atrium. A decrease in the late inferior forces may be evident in lower-loop reentry, because of wave front collision in the lateral right atrium. With multiple or variable wave front breaks in the lateral atrium, unusual and changing ECG patterns may be observed. Alteration of P wave polarity from positive to negative in V<sub>1</sub> may occur.<sup>26</sup> CW lower-loop reentry typically demonstrates positive flutter waves in the inferior leads and negative flutter waves in V<sub>1</sub>.

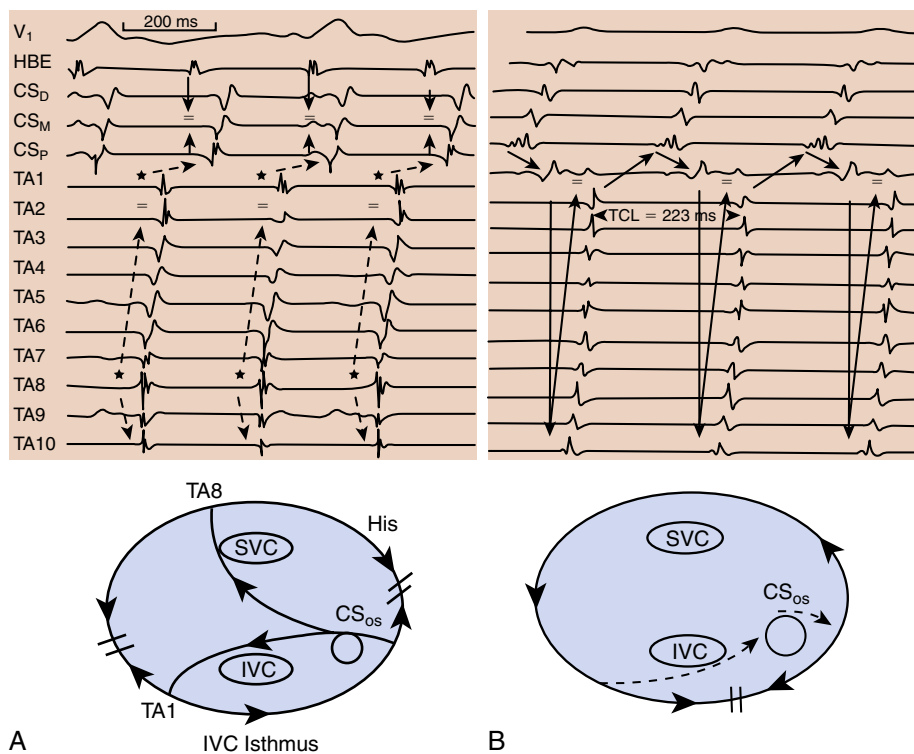


**Fig. 11.4** Electrograms and schematic representation of atrial activation in lower-loop reentry and partial isthmus-dependent flutter. A, During lower-loop reentry, the posterior right atrium is part of the reentry circuit around the inferior vena cava, and wave fronts collide in the lateral right atrium. The electrograms show multiple collisions at recording sites on the lateral right atrial wall TA1 and TA8 (stars). B, During partial isthmus-dependent flutter, the wave front bypasses the anterior CTI near the TVA by passing through the Eustachian ridge posterior to the coronary sinus ostium (CS<sub>os</sub>). The coronary sinus ostium is activated prematurely, and the tachycardia is not entrained from the medial CTI itself. IVC, Inferior vena cava; SVC, superior vena cava; TA10, proximal recording electrodes on halo catheter near upper septum; TA1, distal recording electrodes on Halo catheter near lateral aspect of the CTI. (From Yang Y, Cheng J, Bochoeyer A, et al. Atypical right atrial flutter patterns. *Circulation*. 2001;103:3092-3098. With permission.)

The ECG description of partial isthmus-dependent flutter is incomplete, but it may be expected to resemble typical AFL, given their similar patterns of atrial activation.<sup>25</sup>

The surface ECG pattern of IIR is variable, with 86% of cases resembling typical CCW AFL and 21% of cases exhibiting atypical AFL (positive F waves in inferior leads and V1). In the majority of patients with IIR (79%), a distinct isoelectric period was observed between surface F waves, which were often low amplitude or flat.<sup>27-29</sup>

### Electrophysiologic Diagnosis

Despite the utility of the 12-lead ECG in making a presumptive diagnosis of typical AFL, an electrophysiologic study with mapping and entrainment should be performed to confirm the underlying mechanism if RFCA is to be successfully performed (see Table 11.1). This is particularly true in the cases of reverse typical AFL or CTI-dependent flutter following left atrial ablation, which are much more difficult to diagnose on 12-lead ECG.

For the electrophysiologic study of AFL, activation mapping may be performed using multielectrode catheters or 3-dimensional electroanatomic computerized activation mapping systems. For standard multielectrode catheter mapping, catheters are positioned in the right atrium, His bundle region, and CS. To most precisely elucidate the endocardial activation sequence, a duo-decapolar catheter (e.g., Halo 20-electrode mapping catheter) may be positioned in the right atrium around the TVA (Fig. 11.7). These catheters may extend to the lateral

CTI or cross the entire CTI into the CS, depending on design. The latter obviates the need for a separate CS catheter. Recordings obtained during AFL from all electrodes are then analyzed to determine the right atrial activation sequence.

For patients who present to the laboratory in sinus rhythm, it is necessary to induce AFL to confirm its mechanism. Induction of AFL is accomplished by atrial programmed stimulation or burst pacing, usually from the CS ostium or low lateral right atrium. The direction of AFL induced (e.g., CCW vs. CW) may depend in part on the pacing site. For burst pacing, cycle lengths between 180 and 240 ms are typically effective in producing unidirectional CTI block and inducing AFL. Induction of AFL typically occurs immediately after the onset of unidirectional CTI isthmus block, or after a brief period of rapid atrial tachycardia or atrial fibrillation.<sup>24</sup> During electrophysiologic study, a diagnosis of either typical or reverse typical AFL is suggested by observing a CCW or CW activation pattern in the right atrium around the TVA, respectively. For example, as seen in Fig. 11.8, A in a patient with typical AFL, the initial atrial activation is recorded at the CS ostium (i.e., CS os EGM), which is timed with the initial down stroke of the F wave in the inferior surface ECG leads, followed by caudal-to-cranial activation in the interatrial septum (i.e., His bundle atrial EGM), then cranial-to-caudal activation in the right atrial free wall (i.e., proximal to distal EGMs on the duo-decapolar catheter), and finally to the CTI (i.e., ablation catheter atrial EGM), demonstrating that the underlying mechanism is a CCW macroreentry circuit around

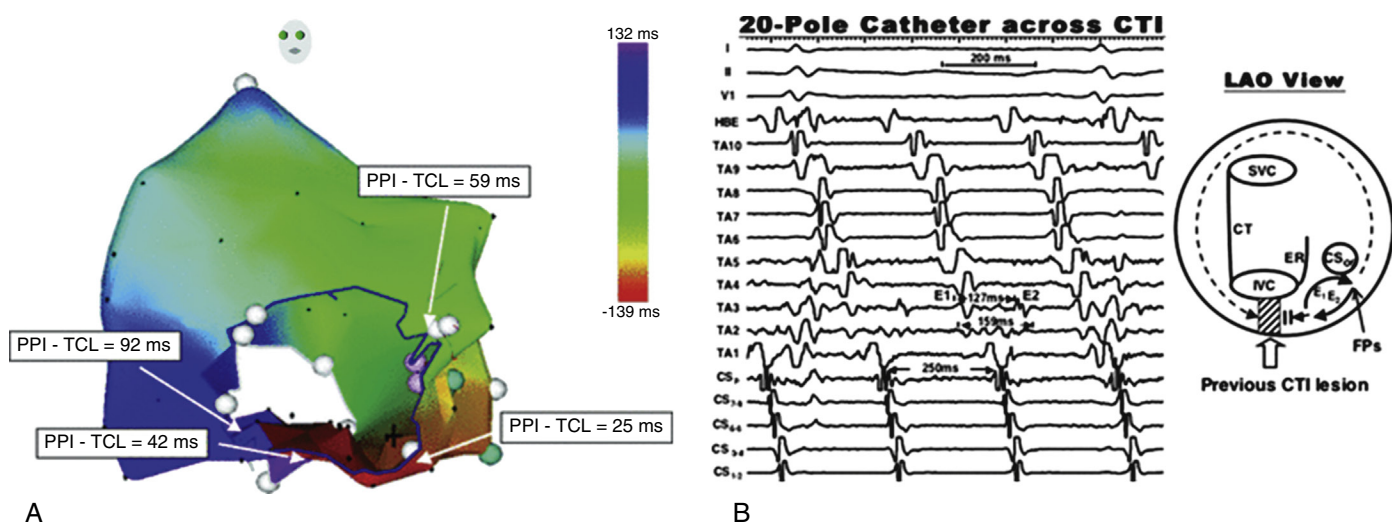


**Fig. 11.5** A, A CARTO map in a patient with typical atrial flutter (AFL) with a counterclockwise activation sequence around the tricuspid valve annulus (TVA). In the left anterior oblique (LAO) view, the earliest activation was at the septal cavotricuspid isthmus (CTI) and latest activation at the lateral CTI, resulting in an “early meets late” activation pattern at the CTI. The mapped cycle length spanned 99% of the tachycardia cycle length (TCL). However, the postpacing interval (PPI)-TCL interval, measured at different sites around the TVA, showed that only the septal CTI was in the circuit. B, Simultaneous surface electrocardiogram recordings (leads I, II, and V1), a His bundle (HBE), coronary sinus (CS), and duo-decapolar catheter positioned around the TVA, with its distal electrode (TA1) across the CTI at CS ostium and proximal electrode (TA10) close to the high lateral TVA in a patient with typical AFL (cycle length 250 ms). The electrodes TA1–3 were located within the septal CTI (from the CS ostium to 6:00 o’clock on the TVA). Note the low amplitude fractionated potentials (FPs) with a duration of 159 ms, recorded at TA2, which spanned 64% of the TCL, and the double potentials (DPs) with E1 to E2 interval of 127 ms recorded at TA3. A combination of the recordings from TA1 to TA3 (i.e., both FPs and DPs) spanned more than 2/3 of the TCL. In this patient, entrainment pacing from the septal CTI during the tachycardia showed a PPI-TCL  $\leq$  25 ms, whereas pacing from the lateral CTI showed a PPI-TCL greater than 25 ms. Radiofrequency catheter ablation at the septal CTI, where the FPs were recorded, terminated the AFL, and it was no longer inducible after ablation. The schematic diagram to the right of the figure shows the proposed reentrant circuit. (From Yang Y, Varma N, Badhwar N, et al. Prospective observations in the clinical and electrophysiologic characteristics of intra-isthmus reentry. *J Cardiovasc Electrophysiol*. 2010;21:1099-106. With permission.)

**TABLE 11.1 Diagnostic Criteria for Isthmus-Dependent Flutters**

Type of Flutter	Criteria
<b>Surface ECG</b>	
Typical flutter	Saw tooth upright F wave pattern in the inferior ECG leads and in V1
Reverse typical flutter	Sine wave or upright F wave pattern in the inferior ECG leads
Lower loop reentry	Variable; often resembles typical flutter if counterclockwise; clockwise rotation usually yields upright F waves inferriorly and inverted in V1
Partial-isthmus reentry	Poorly described; probably similar to typical flutter
<b>Electrophysiologic Testing</b>	
Isthmus-dependent flutters	Demonstration of entrainment criteria during pacing from the CTI, Including the following: First postpacing interval <30 ms longer than tachycardia cycle length Stimulus-to-F-wave interval equal to electrogram-to-F-wave interval on pacing catheter Identical paced F wave morphology and atrial activation sequence Macroreentrant RA activation by standard activation or electroanatomic mapping with entire tachycardia cycle length represented in right atrium
Typical flutter	Concealed entrainment from CTI and counterclockwise macroreentrant RA activation
Reverse typical flutter	Concealed entrainment from CTI and clockwise macroreentrant RA activation
Lower loop reentry	Concealed entrainment from both CTI and low posterior right atrium with clockwise or counterclockwise macroreentrant RA activation
Partial isthmus-dependent	Concealed entrainment from lateral but not medial margin of CTI; early coronary sinus ostium activation during flutter; wave front collision in CTI; counterclockwise macroreentrant RA activation

CTI, Cavotricuspid isthmus; ECG, electrocardiogram; RA, right atrial.

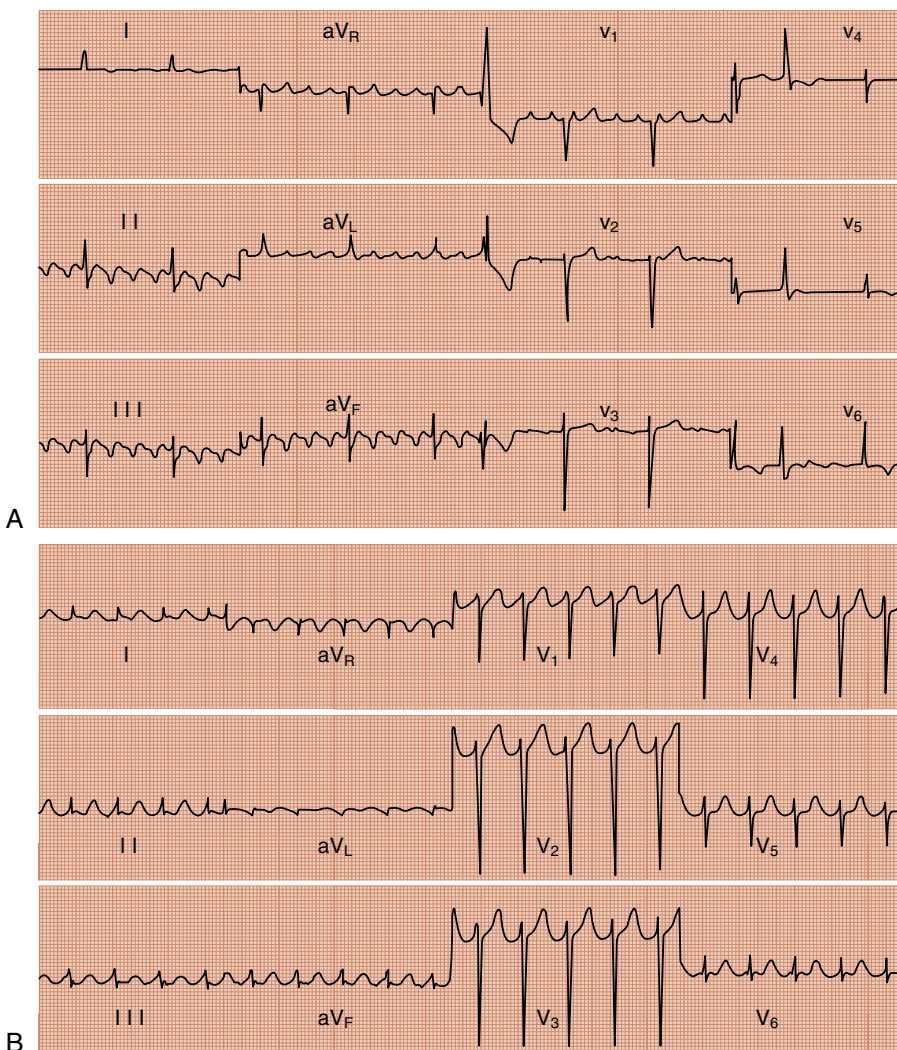


**Fig. 11.6** A, A 12-lead electrocardiogram recorded during typical atrial flutter (AFL). Note the sawtooth F wave pattern in the inferior leads II, III, and aVF. Typical AFL is also characterized by flat to biphasic F waves in I and aVL, respectively; an upright F wave in V<sub>1</sub>; and an inverted F wave in V<sub>6</sub>. B, A 12-lead electrocardiogram from a patient with the reverse typical AFL. The F wave in reverse typical AFL has a less distinct, sine-wave pattern, in the inferior leads. In this case, the F waves are upright in the inferior leads II, III, and aVF; biphasic in leads I, aVL, and V<sub>1</sub>; and upright in V<sub>6</sub>.

the TVA encompassing the entire tachycardia cycle length. In a patient with reverse typical AFL, the mirror image of this activation pattern is seen (see Fig. 11.8 B).

In addition, confirmation that the AFL reentry circuit uses the CTI, requires demonstration of classical criteria for entrainment, including concealed entrainment, during pacing from the CTI, and constant fusion from a site or sites outside the CTI (often the lateral right atrium).<sup>5</sup> Criteria for demonstrating concealed entrainment of AFL include acceleration of the tachycardia to the pacing cycle length without a change in the F wave pattern on surface ECG or endocardial atrial activation pattern and EGM morphology, as well as immediate resumption of the tachycardia at the original cycle length on termination of pacing, including the first postpacing interval (i.e., the post-pacing interval minus tachycardia cycle length, or PPI-TCL), should be less than 30 ms, (Fig. 11.9). Concealed entrainment is further confirmed, during pacing from the CTI, if the stimulus-to-F-wave or stimulus-to-reference EGM interval during pacing, and the pacing electrode EGM-to-F-wave or pacing EGM-to-reference EGM interval during AFL are the same (see Fig. 11.9). Furthermore, during typical

AFL, the stimulus-to-F-wave or stimulus-to-proximal CS EGM is shorter when the pacing site is medial, near the exit from the CTI (e.g., 30 to 50 ms), and longer when the pacing site is lateral, near the entrance to the CTI (e.g., 80–100 ms). The converse is true during reverse typical AFL. In contrast, pacing at sites outside the CTI results in manifest entrainment of AFL, with progressive fusion of the F post-pacing interval wave pattern and endocardial atrial EGMs at progressively shorter cycle lengths faster than the AFL cycle length.

The diagnosis of lower loop reentrant AFL is confirmed by demonstration of concealed entrainment of the tachycardia from not only the CTI but also the inferior-posterior right atrium.<sup>25</sup> Partial isthmus-dependent flutter is confirmed by the demonstration of concealed entrainment from the lateral margin of the CTI but not from the medial portion near the TVA. In addition, there is early activation of the CS ostium and evidence of wave front collision within the medial CTI. Concealed entrainment should be demonstrable from the area of short circuit between the Eustachian ridge and CS ostium.

The diagnosis of IIR is confirmed by demonstration of concealed entrainment only within the septal CTI near the CS ostium, while all

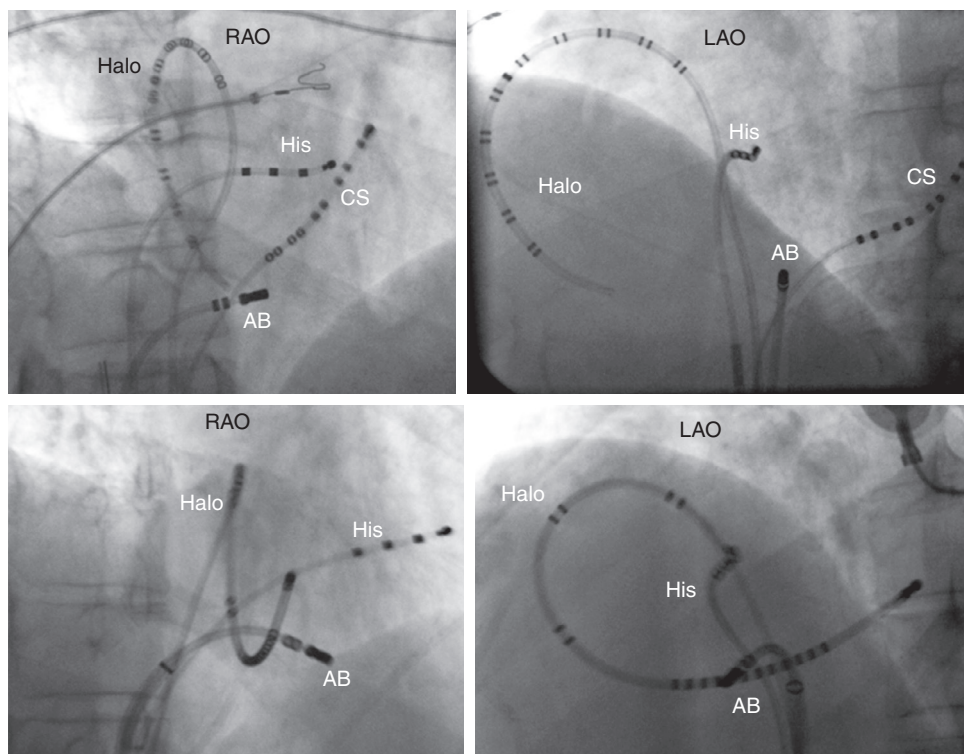


**Fig. 11.7** Right anterior oblique (*left panel*) and left anterior oblique fluoroscopic (*right panel*) projections showing the intracardiac positions of the His bundle (His), coronary sinus (CS), halo (Halo), and ablation catheters (AB). Two types of multielectrode mapping catheters are shown. *Top*, This design does not span the cavotricuspid isthmus (CTI). In this patient, the ablation catheter is septal and withdrawn to the posterior CTI near the inferior vena cava. *Bottom*, This design spans the CTI with closely spaced electrodes and continues into the coronary sinus. In this patient, the ablation catheter is over the central part of the CTI near the tricuspid valve annulus.

other areas of the right atrium, left atrium, and CS are out of the circuit ( $\text{PPI-TCL} > 25$ )<sup>27,28</sup>. In addition, fractionated potentials and double potentials are often observed within the septal area of the CTI. In rare instances, concealed entrainment and fractionated potentials have also been observed at the mid or antero-inferior CTI, indicating extension of the circuit more laterally. Electroanatomic mapping may not have adequate resolution to identify this microreentrant circuit. It may demonstrate either a focal pattern with total mapped cycle length less than 60% of the tachycardia cycle length with earliest activation arising from the septal CTI near the CS ostium, or it may demonstrate a CCW reentrant pattern around the TVA, with the total mapped cycle length greater than 90% of the TCL, deceptively suggesting the presence of typical CTI-dependent AFL.

The differential diagnosis of AFL from other supraventricular arrhythmias is usually apparent given typical ECG manifestations and variable ventriculoatrial relationships. The most important distinction to be made is the exclusion of a focal atrial tachycardia. Rarely, focal atrial tachycardia in the low posteroseptal right atrium may be confused with AFL if unidirectional CTI conduction block (i.e., medial to lateral block) is present. Otherwise, the atrial tachycardia can be recognized by failure to entrain it from the CTI and by a radial activation pattern.

## ABLATION

For ablation of CTI-dependent AFL, the most common approach is to create a line of bidirectional conduction block across the CTI, from the TVA to the IVC. For this purpose, a variety of mapping and ablation

catheters, with different shapes and curve lengths, as well as RF generators, are available from several commercial manufacturers.<sup>2–4,6,32–34</sup> We prefer to use a standard-curve ablation catheter (Blazer™ 8-mm tip, mid-distal standard curve, Boston Scientific, Inc., Natick, MA, USA) or an externally irrigated ablation catheter (Thermocool ST™, Biosense Webster, Diamond Bar, CA, USA; Tacticath, Abbott Laboratories, Chicago, IL, USA) because it has been shown that the use of large-tip (8–10 mm) ablation catheters or irrigated ablation catheters reduces procedure durations and improves success rates compared with standard 4-mm RF electrodes.<sup>35–37</sup> The smaller electrode (3.5 mm) on irrigated catheter designs may provide better near-field EGM resolution than large-tip electrodes as well. Long, fixed-curve guide sheaths (e.g., SR0 or SL1, St. Jude, Inc., St. Paul, MN, USA) or steerable deflectable sheaths (e.g., Agilis, St. Jude, Inc., St. Paul, MN, USA) are also useful to improve catheter reach, stability, and tissue contact. There is also published evidence that large-tip ablation catheters are most useful for flat CTI anatomy, whereas irrigated designs may be more advantageous in the presence of CTI pouches.<sup>38</sup> When using fixed curve or steerable sheaths, it is important that the curvatures of the sheath and catheter remain coaxial. Paradoxically, rotating the sheath to point into the septum may limit the septal motion of the catheter.

The target for CTI-dependent AFL ablation is the CTI (Table 11.2), which when standard multipolar electrode catheters are used for mapping and ablation, is localized with a combined fluoroscopically and electrophysiologically guided approach.<sup>2–4,6,32–42</sup> The usual target for the ablation line is the central isthmus because the CTI is narrowest at this point (i.e., distance from TVA to IVC) and has the thinnest musculature.<sup>15</sup> This site is located at 6 o'clock in the LAO view (see

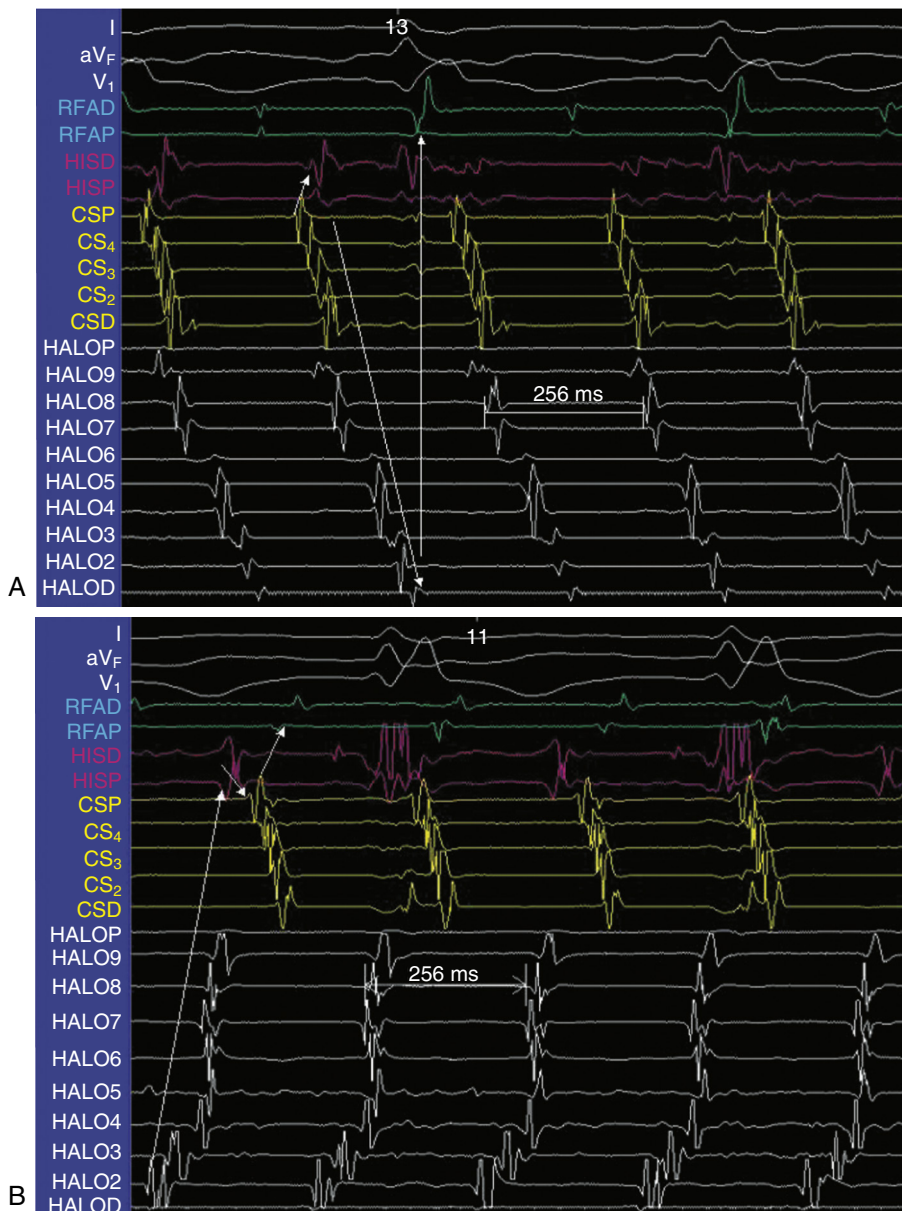


**Fig. 11.8** Endocardial electrograms from the mapping and ablation, multielectrode Halo, coronary sinus (CS), and His bundle catheters and surface electrocardiogram leads I, aVF, and V<sub>1</sub>, demonstrating a counterclockwise rotation of activation in the right atrium in a patient with typical atrial flutter (AFL) (A) and a clockwise rotation of activation in the right atrium in a patient with reverse typical AFL (B). The cycle length was 256 ms for both the typical and reverse-typical forms of AFL. Arrows demonstrate the activation sequence. The HALOD through HALOP tracings are 10 bipolar electrograms recorded from the distal (low lateral right atrium) to the proximal (high right atrium) poles of the 20-pole Halo catheter positioned around the tricuspid valve annulus, with the proximal electrode pair at 1 o'clock and the distal electrode pair at 7 o'clock. CSP electrograms were recorded from the CS catheter proximal electrode pair positioned at the CS ostium, HISP electrograms from the proximal electrode pair of the His bundle catheter, and RFAD electrograms from the mapping and ablation catheter positioned with the distal electrode pair in the cavotricuspid isthmus.

[Fig. 11.7](#)). One drawback to ablation of the central isthmus is the frequent occurrence of pouches in this region. Pouches may be avoided by ablating the lateral isthmus (7 o'clock in LAO projection). However, there are thicker right atrial musculature and terminal pectinate muscles found here. The medial isthmus is devoid of pectinate musculature but contains the thickest atrial muscular layer and is nearest to the right coronary artery and AV nodal extensions. Typically, the ablation catheter is positioned using fluoroscopic guidance (see [Fig. 11.7](#)) or

electroanatomic mapping, in the central CTI, with the distal ablation electrode on or near the TVA in the right anterior oblique (RAO) view, and midway between the septum and low right atrial free wall (6- or 7 o'clock position) in the LAO view. The distal ablation electrode position is then adjusted toward or away from the TVA, based on the ratio of atrial and ventricular EGM amplitudes (A/V ratio) recorded by the bipolar ablation electrode. An optimal ratio is 1:2 or 1:4 at the TVA, as seen in [Fig. 11.8](#), A on the ablation electrode. After the ablation catheter

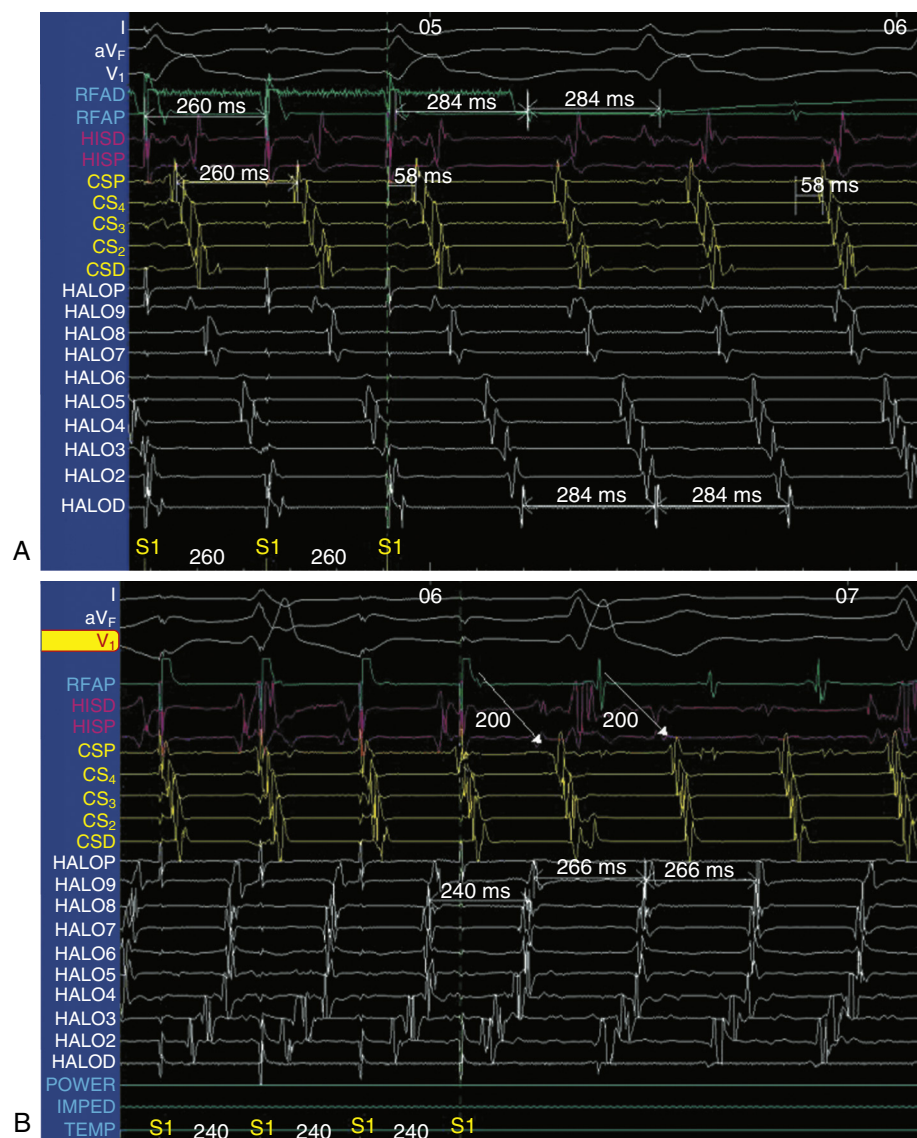


**Fig. 11.9** Surface electrocardiogram (ECG) and endocardial electrogram (EGM) recordings during pacing entrainment from the cavotricuspid isthmus in patients with both typical atrial flutter (AFL) (A) and reverse-typical AFL (B). Note in both examples that the tachycardia is accelerated to the pacing cycle length and that the F wave morphology on surface ECG and endocardial waveforms and the endocardial activation pattern are unchanged during pacing compared with AFL, indicating concealed entrainment. Furthermore, the stimulus-to-F-wave or local EGM intervals are comparable to the EGM-to-F-wave or local EGM intervals recorded on the mapping and ablation catheter (RFAD) during entrainment and AFL in both examples, indicating concealed entrainment. Halo catheter tracings are as described in Fig. 11.7. CS, Coronary sinus; S1, pacing stimulus artifact.

**TABLE 11.2 Targets for Ablation of Isthmus-Dependent Flutters**

Type of Flutter	Targets
CTI-dependent	CTI from TVA to IVC TVA to Eustachian ridge isthmus TVA to CS ostium to Eustachian ridge isthmus Maximal electrogram voltage recorded on-line
Partial isthmus-dependent	CS ostium to IVC

CS, Coronary sinus; CTI, cavotricuspid isthmus; IVC, inferior vena cava; TVA, tricuspid valve annulus.

is positioned on or near the TVA, it is very slowly withdrawn during ablation toward the IVC while RF energy is applied continuously.

Alternatively, the ablation catheter can be withdrawn in a stepwise manner, a few millimeters at a time (usually less than or equal to the length of the distal ablation electrode), with 30- to 60-second pauses at each location, during a continuous or interrupted energy application. For irrigated electrodes, a maximal power of 35 to 50 W and a temperature of 40°C to 45°C should be used.<sup>35–38</sup> In contrast, the large-tip (i.e., 8–10 mm) ablation catheters require a higher power, up to 100 W, to achieve target temperatures of 50°C to 60°C, because of the greater energy-dispersive effects of the larger ablation electrode. Use of large-tip ablation catheters also requires the use of two grounding pads applied to the patient's skin to avoid skin burns.<sup>38,40–42</sup> Excessive impedance drops (i.e., >10–20 Ω from baseline) should be avoided, to prevent tissue overheating and steam pops. CTI ablation can be performed with standard 4-mm-tipped RF catheters (50 W, 50–65°C); however, use of these catheters is associated with longer procedure and ablation times, lower acute success rates, and much higher recurrence rates. EGM recordings may be used in addition to fluoroscopy to ensure that the ablation electrode is in contact with viable tissue in the CTI throughout each energy application. However, recent studies have suggested that real-time contact force measuring catheters may help reduce total ablation time required to produce acute CTI conduction block, and that standard surrogates of tissue contact (e.g., impedance, EGM amplitude) may not ensure adequate tissue contact during ablation as measured by contact force sensing catheters.<sup>43–44</sup>

Ablation across the entire CTI (Fig. 11.10) may require several sequential 30- to 60-second energy applications during a stepwise catheter pullback, or a prolonged energy application of up to 120 seconds or longer during a continuous catheter pullback. The catheter should be gradually withdrawn until the distal ablation electrode no longer records an atrial EGM, indicating that it has reached the IVC, or until the ablation electrode is noted to abruptly slip off the Eustachian ridge. RF energy application should be immediately interrupted when the catheter has reached the IVC, because ablation in extracardiac venous structures is known to cause significant pain. Computerized 3-dimensional mapping systems are useful to document the anatomic placement of ablation lesions and decrease fluoroscopy use.<sup>45</sup> As the ablation catheter approaches the IVC, it is often useful to release the catheter curve slightly and withdraw the sheath and catheter as a unit to allow greater contact between the electrode and the CTI, before the catheter is withdrawn into the IVC.

Ablation of the TV-CS and CS-IVC isthmuses (see Fig. 11.10) may also be performed, using an approach similar to that used for CTI ablation.<sup>46</sup> However, for this approach to be successful, it may be necessary to ablate within the CS ostium, which may be associated with a higher risk of complications such as atrioventricular (AV) node block. It has also been reported that CTI-dependent AFL may be cured by ablating between the TVA and Eustachian ridge only, which is a narrower isthmus than the CTI.<sup>47</sup>

During repeat ablation, it may be necessary to rotate the ablation catheter away from the initial line of energy application, either medially or laterally in the CTI, to create new or additional lines of block, or to use a higher power or higher ablation temperature, or both. In addition, if ablation is initially attempted using a standard 4- to 5-mm-tip electrode and fails, repeat ablation with a large-tip electrode catheter or a cooled-tip ablation catheter may be successful.<sup>35–42</sup> Ablation of partial isthmus-dependent flutter requires creation of a line of block from the CS ostium to the IVC, eliminating conduction across the Eustachian ridge. Completion of this line may convert the tachycardia to typical isthmus-dependent flutter, which then requires ablation of the entire CTI.<sup>25</sup>

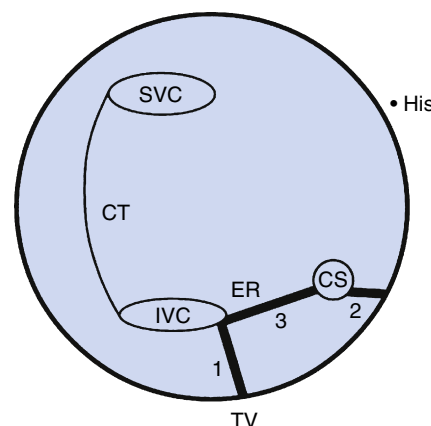


**Fig. 11.10** Schematic diagram of the right atrium in the right anterior oblique view, showing the typical locations for linear ablation of the cavotricuspid isthmus (line 1), the tricuspid valve (TV)–coronary sinus (CS) isthmus (line 2), and the CS–inferior vena cava (IVC) isthmus (line 3). CT, crista terminalis; ER, Eustachian ridge; His, His bundle; SVC, superior vena cava.

In many cases, the CTI is composed of discrete muscle bundles embedded within connective tissue. Therefore a continuous ablation line may be unnecessary to achieve conduction block. To reduce procedure times and unnecessary ablation, the maximal voltage-guided CTI technique has been introduced.<sup>48,49</sup> Bipolar EGMs are recorded from the ablation catheter in the central CTI during AFL or during CS pacing. As the catheter is withdrawn from the TVA to the IVC, the locations with the largest peak-to-peak bipolar voltage are marked. The ablation catheter is then returned to those sites of maximal voltage, and RF energy is delivered for 60 seconds or until there is more than 50% reduction in the EGM voltage. The line is then remapped for the largest remaining EGM voltage and the procedure repeated until CTI block is confirmed. In randomized trials, the voltage-guided technique has been reported to reduce ablation time, number of lesions, and procedure and fluoroscopy times compared with the conventional anatomic approach.<sup>48,49</sup> However, whether such a limited approach will yield high long-term outcome results has not been studied.

After the termination of flutter, less than half of patients demonstrate bidirectional CTI block, and further ablation is often needed.<sup>50</sup> Persistent CTI conduction can be detected by pacing medial (i.e., proximal coronary sinus) or lateral (i.e., low lateral right atrium) to the ablation line and mapping the line for conduction gaps. The presence of split EGMs with less than 90 ms between EGM components is suggestive of a conductive gap in the line.<sup>50</sup> As the line is systematically mapped, the split EGM components draw closer together as the gap is approached. The gap itself is identified as a single or fractionated potential along the line bounded by split EGMs (Fig. 11.11).

Ablation of the CTI for AFL has also been performed using a linear microwave ablation catheter system (Medwaves, Inc., Rancho Bernardo, CA, USA) with antenna lengths up to 4 cm.<sup>51</sup> These studies have shown the feasibility of linear microwave ablation of the CTI, which has the potential advantage of rapid ablation of the CTI with a single energy application over the entire length of the ablation electrode (Fig. 11.12).

Computerized 3-dimensional-mapping systems provide several advantages for CTI ablation but are not required for the procedure.<sup>45</sup> Electroanatomic mapping before ablation can demonstrate the reentry circuit, thus supporting the diagnosis (Fig. 11.13). In addition, 3-dimensional anatomic reconstruction may identify the presence of a CTI pouch, and high-voltage EGMs may indicate the presence of pectinate muscle extension into the CTI. During ablation, 3-dimensional mapping systems

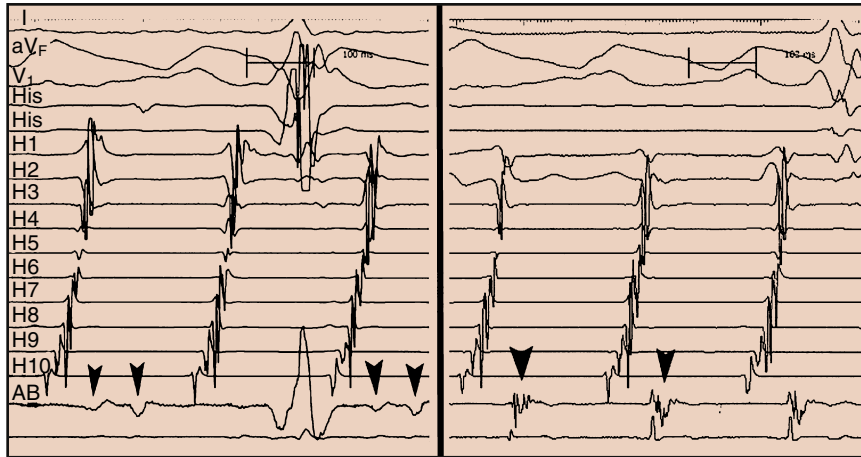


**Fig. 11.11** Mapping for a gap in the ablation line in the cavotricuspid isthmus. In this patient, a previous attempt to terminate typical atrial flutter (AFL) had failed. *Left panel*, The ablation catheter (AB) records low-amplitude split electrograms (EGMs) (arrowheads) along the prior ablation line. The interval between EGM components was 70 ms during AFL. *Right panel*, With further interrogation of the ablation line, a site with a single-component, fractionated EGM (arrowheads) was identified. Ablation at this site terminated AFL in less than 2 seconds and created bidirectional block. Surface electrocardiogram leads I, aVF, and V<sub>1</sub> are shown. *His*, His channels; *H1* through *H10*, halo catheter channels from distal to proximal.

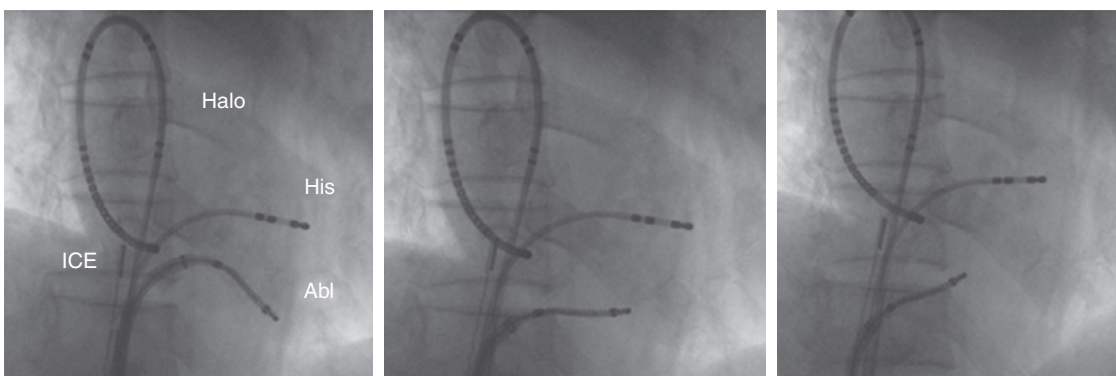


**Fig. 11.12** Fluoroscopic right anterior oblique view of the Medwaves, Inc., microwave ablation (Abl) antenna positioned across the cavotricuspid isthmus (CTI). Left panel shows ablation antenna positioned near the tricuspid valve annulus (TVA). Middle panel shows ablation antenna at the middle CTI between the TVA and Eustachian ridge. Right panel shows ablation antenna withdrawn near the inferior vena cava. *Halo*, Halo catheter; *His*, His bundle; *ICE*, intracardiac echocardiography.

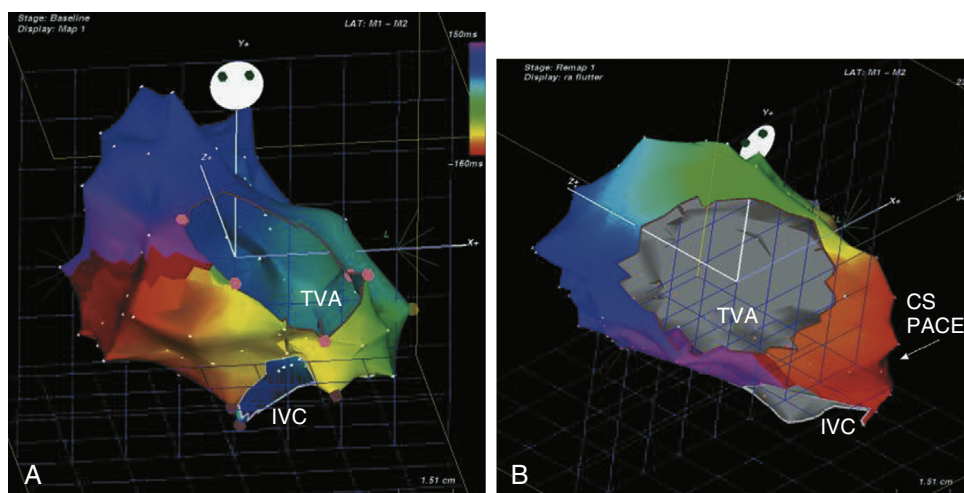


**Fig. 11.13** A 3-dimensional electroanatomic (Carto system, Biosense Webster, Diamond Bar, CA) map of the right atrium in a patient with typical atrial flutter (AFL), before (A) and after (B) Cavotricuspid isthmus (CTI) ablation. Note the counterclockwise activation pattern around the TVA during AFL (A, anteroposterior view), which is based on a color scheme indicating activation time from orange (early) to purple (late). After ablation of the CTI (B, left anterior oblique caudal view), during pacing from the coronary sinus (CS) ostium, there is evidence of medial-to-lateral CTI conduction block, as indicated by juxtaposition of orange and purple color in the CTI. *IVC*, Inferior vena cava; *TVA*, tricuspid valve annulus.

allow for documentation of each ablation lesion delivered, which may be helpful to complete an anatomically based ablation line and identify areas of anatomic gaps. Computerized mapping systems may therefore reduce fluoroscopy times by 50%, compared with conventional approaches.<sup>45</sup> After ablation, detailed electroanatomic mapping may be used to confirm the presence of CTI block or slow conduction as well.

Unlike typical AFL, reverse-typical AFL, lower-loop reentry, and partial isthmus flutter whose circuits all involve the lateral and central CTI, the ablation approach for IIR is slightly modified to interrupt the circuit located in the septal or medial CTI.<sup>27,28</sup> Successful ablation should be achieved by identifying and ablating the site with the longest fractionated potential associated with concealed entrainment and completing a septal CTI line from the tricuspid annulus to the IVC that includes this site.

### Overcoming Difficult Cavotricuspid Isthmus Anatomy

The complex anatomy of the CTI may in some cases present difficulties for ablation. The most common problems encountered are the presence of a large CTI pouch, large pectinate muscles, and/or a prominent Eustachian ridge.<sup>52</sup> A pouch is a deep recess in the CTI, that may be skipped over by the ablation electrode during pullback (Fig. 11.14). The junction of the IVC and Eustachian ridge may form a “fulcrum” for the ablation catheter (see Fig. 11.14), preventing the distal ablation electrode from achieving adequate contact with the CTI, especially if there is a pouch in the CTI. The presence of a pouch may be identified by preprocedure CT or MRI, or more commonly by intracardiac echocardiography (ICE) or electroanatomic mapping, during the procedure. Right atrial angiography

to identify CTI anatomy may also be performed by injecting 50 mL of contrast over 3 to 5 seconds through a 5 F pigtail catheter in the upper IVC or IVC-right atrial junction,<sup>18</sup> while imaging in the RAO view. A CTI pouch may be avoided by a more lateral ablation line. Ablation within a CTI pouch may be accomplished by forming a 180-degree curvature on the ablation catheter (i.e., so-called “knuckle maneuver”) in the mid-tricuspid annulus and withdrawing the catheter to enter the pouch perpendicularly (Fig. 11.15). The curvature can be relaxed or tightened to reach the TVA and IVC ends of the pouch, respectively. Because of the restricted blood flow that may occur in a pouch, care should be taken to avoid excessive tissue heating and steam pops.

Large pectinate muscles should be suspected when recording high-voltage EGMs within the CTI during 3-dimensional electroanatomic mapping. These may potentially be avoided by ablation in the medial isthmus. Ablation of the high-voltage areas may require protracted (60–120 seconds) RF delivery. On the trabecular prominences, catheter contact may be unstable, whereas in the trabecular valleys, excessive electrode temperatures may result in steam pops (Fig. 11.16).<sup>52</sup> Preformed or deflectable sheaths may enhance tissue contact, and for irrigated ablation, lesion sizes are maximized with the electrode perpendicular to the tissue. And as noted earlier, a voltage-guided approach may limit unnecessary ablation.

A prominent Eustachian ridge can be detected by angiography or ICE (Fig. 11.17). The Eustachian ridge and adjacent tissue can be conductive and require ablation. Not only may the Eustachian ridge cause a fulcrum effect limiting distal ablation electrode contact with parts of the CTI as noted earlier, it may actually shield parts of the

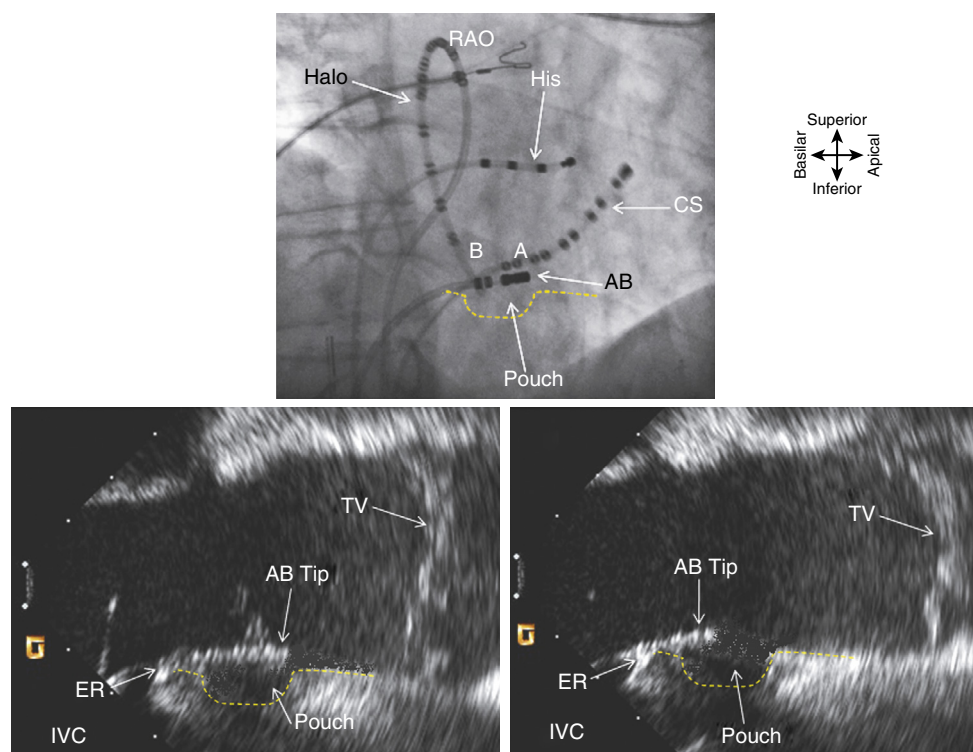


**Fig. 11.14** A cavotricuspid isthmus (CTI) pouch is shown in this figure. *Top panel*, Right anterior oblique (RAO) fluoroscopic view of ablation catheters during CTI ablation. The yellow dashed line estimates the position of a large pouch visualized in this patient with intracardiac echocardiography (ICE) (*bottom panels*). As the ablation (AB) catheter is drawn toward the inferior vena cava (IVC) from point A to B, the tip of the catheter does not contact the floor of the pouch, and it is therefore not ablated. *Bottom left panel*, This ICE view demonstrates the pouch and ablation catheter skipping over the pouch in position A. The echo view is rotated to correspond to the fluoroscopic view. *Bottom right panel*, This echo image corresponds to the ablation catheter at position B. The fulcrum created by the Eustachian ridge (ER) prevents the catheter from entering the pouch. CS, Coronary sinus catheter; TV, tricuspid valve.

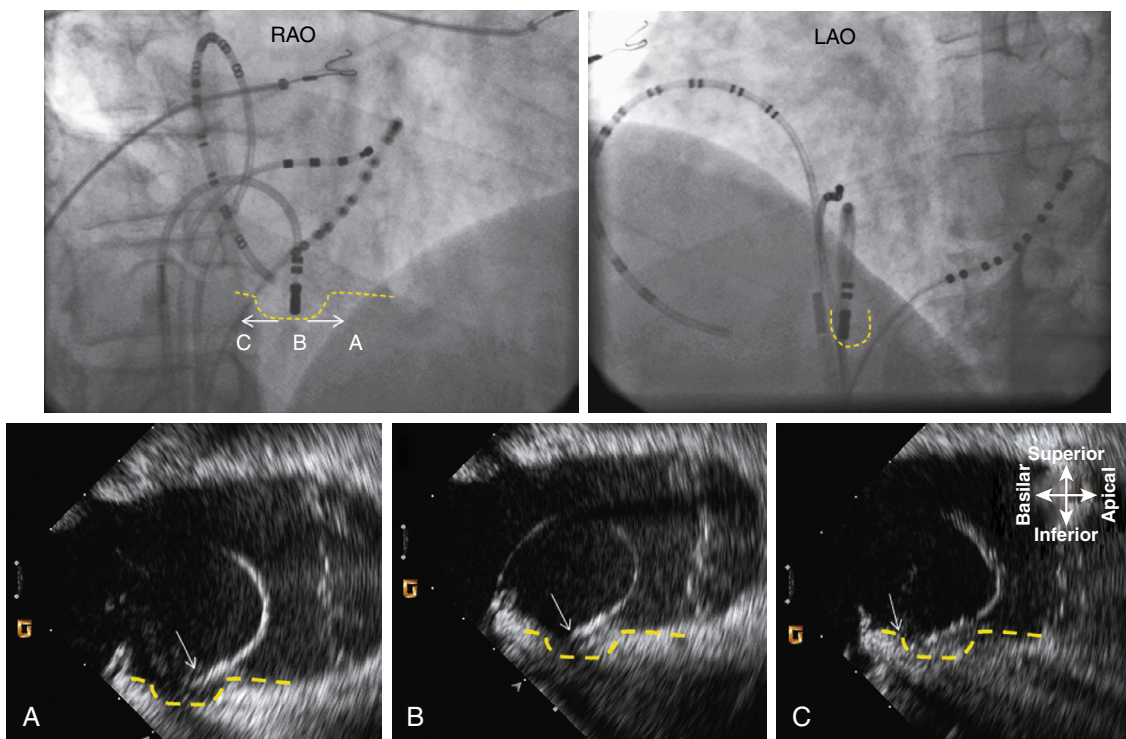


**Fig. 11.15** Ablation within a cavotricuspid isthmus (CTI) pouch is shown in this figure. Top panels show right anterior oblique (RAO) and left anterior oblique (LAO) fluoroscopic views of the catheter positions. The dashed yellow line represents the estimated location of the pouch visualized on intracardiac echocardiography. With a 180-degree angle on the ablation catheter, the ablation electrode contacts the middle floor of the pouch (site B). By opening or closing the curve on the ablation catheter, the tricuspid valve annulus end (site A) and inferior vena cava end (site C) of the pouch can be reached, respectively. Bottoms panels visualize the position of the ablation electrode at sites A, B, and C in the pouch. The arrows indicate the tip of the ablation catheter. The echo views are rotated to correspond to the RAO fluoroscopic image.

CTI entirely from ablation electrode contact (e.g., areas just anterior and below the Eustachian ridge). Again, by using the “knuckle maneuver,” the electrode may be brought into contact with both the IVC and CTI sides of the Eustachian ridge for successful ablation (see Fig. 11.17).<sup>52</sup> This limitation may also be overcome by use of a preformed sheath that directs the catheter anteriorly so that by placing a posterior curvature on the catheter body these areas can be reached (Fig. 11.18).

Occasionally, multielectrode catheters crossing the CTI map prevent contact between the ablation electrode and cardiac tissue (Fig. 11.19). When presented with this problem, the mapping catheter can be removed or the ablation catheter positioned beneath the halo (see Fig. 11.19).

### End Points for Ablation

Ablation may be performed during sustained AFL or during sinus rhythm. If it is performed during AFL, the first end point is its termination during energy application (Fig. 11.20). However, even if AFL terminates, CTI conduction persists in more than half of patients.<sup>50</sup> Therefore the entire CTI ablation should be completed before electrophysiologic testing to confirm bidirectional CTI conduction block. After completion of CTI ablation, as determined by fluoroscopic and electrophysiologic criteria described previously, testing can be performed immediately and repeated after at least 30 minutes to ensure that bidirectional CTI block has been achieved and is persistent (Table 11.3).<sup>2–4,6,32–42,52–54</sup> Some 50% of patients demonstrate recurrent CTI conduction during the ablation procedure after CTI bidirectional

block is initially documented.<sup>53</sup> Most reconnections occur within 10 minutes of initially “successful” CTI block, and multiple recurrences after repeat ablation within the same procedure are not uncommon. Isoproterenol infusion may also unmask transient CTI block.<sup>55</sup> If AFL is not terminated during the first attempt at CTI ablation, the activation sequence and isthmus dependence of the AFL should be reconfirmed and ablation repeated.

If AFL is terminated during ablation, pacing should be done at a cycle length faster than the intrinsic sinus cycle length (e.g., 700 or 600 ms) to confirm bidirectional conduction block in the CTI (Figs. 11.21–11.24). If ablation is done during sinus rhythm, pacing can also be done during energy application to monitor for the development of conduction block in the CTI (Fig. 11.25). The use of bidirectional conduction block as an end point for CTI ablation is associated with a significantly lower recurrence rate of CTI-dependent AFL during long-term follow-up.<sup>56–58</sup>

Conduction in the CTI is typically evaluated after ablation by determining the right atrial activation sequence during pacing from the low lateral right atrium and CS ostium. It is important to pace at relatively slow rates, just above the sinus cycle length, during assessment for CTI block, because conduction block across the CTI may be functional or rate dependent in some cases. Conduction block across the crista terminalis may be functional in some patients as well, and at slow pacing rates conduction across the mid-crista region can result in uncertainty regarding the presence or absence of bidirectional conduction block after CTI ablation.<sup>59–60</sup> Therefore it may be necessary to pace not only from the proximal CS but also adjacent to the ablation line in the CTI,

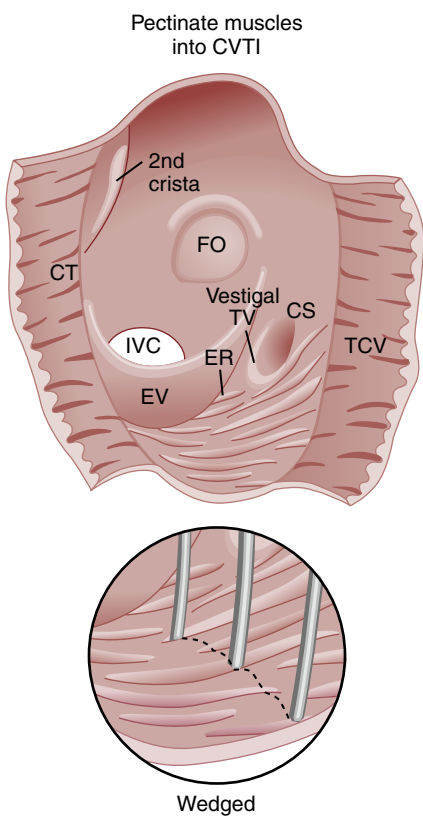


**Fig. 11.16** This illustration demonstrated the potential difficulties in ablating the lateral cavotricuspid isthmus (CTI) in the presence of prominent pectinate muscles. On the tops of the muscle bundles, the catheter contact may be unstable. In the recesses between bundles, electrode overheating and low power delivery may result because of the absence of convective cooling. CS, Coronary sinus; CT, crista terminalis; CVTI, cavotricuspid isthmus; ER, Eustachian ridge; EV, Eustachian valve; FO, foramen ovale; IVC, inferior vena cava; TCV, tricuspid valve. (From Asirvatham S. Correlative anatomy and electrophysiology for the interventional electrophysiologist: right atrial flutter. *J Cardiovasc Electrophysiol*. 2009;20:113-122. With permission.)

or in the posterior-inferior right atrial septum, to confirm the presence of CTI conduction block.<sup>61</sup> Bidirectional conduction block after CTI ablation can be confirmed by demonstrating a cranial-to-caudal activation sequence over the lateral right atrium during pacing from the CS ostium or medial to the ablation line, and a cranial to caudal sequence over the right atrial septum during pacing from the lateral edge of the ablation line or the low lateral right atrium<sup>55-57</sup> (see Figs. 11.21 to 11.24). This sequence can be documented by multielectrode recordings or by electroanatomic 3-dimensional mapping. When using a multipolar electrode catheter to assess CTI block, it is important that the catheter be properly positioned near the TVA. Recordings are needed from immediately adjacent to the ablation line to assess for incomplete block or slow conduction through the ablation line. This can be performed using the multielectrode catheter crossing the ablation line or from the ablation catheter. A misleading activation sequence may be recorded if portions of the mapping catheter extend posterior to the crista terminalis or if the distal ablation electrode is posterior to the Eustachian ridge.<sup>52</sup> In addition, during pacing medial to the ablation line, conduction posterior to the IVC can lead to the appearance of both pseudo-conduction and pseudo-block through the CTI (Fig. 11.26).<sup>52,62</sup> In the case of pseudo-block, conduction from the medial pacing site (usually proximal coronary sinus) may conduct rapidly posterior to the IVC to activate the lateral CTI from lateral to medial, suggesting medial to lateral

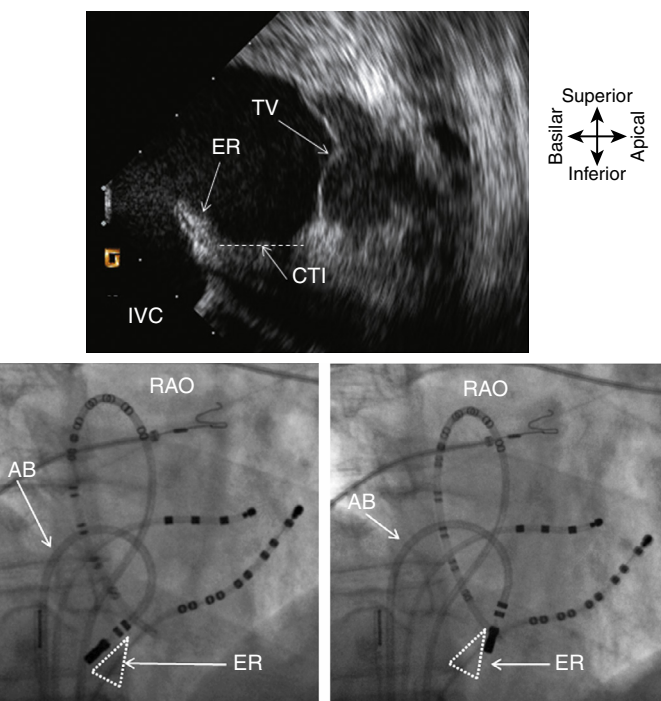


**Fig. 11.17** Ablation of the Eustachian ridge is shown in this figure. The top panel shows a prominent Eustachian ridge (ER) on intracardiac echocardiography. The echo views are rotated to correspond to the right anterior oblique (RAO) fluoroscopic image. Bottom panels show the estimated location of the ER and acute flexion of the ablation (AB) catheter to ablate both aspects of the ER facing the inferior vena cava (IVC; lower left) and tricuspid valve (lower right). TV, Tricuspid valve.

isthmus block despite persisting slow conduction through the isthmus. In this case, detailed mapping along the ablation line should identify gaps in the line. In the case of pseudo-conduction, the posteriorly conducted wave front activates the distal multielectrode mapping catheter in a CW pattern even when there is CTI block. This is more likely to be seen if the distal electrodes on the multielectrode mapping catheter are displaced laterally and do not record from the immediate edge of the ablation line.<sup>52</sup> Pseudo-conduction can be recognized by detailed mapping of sites spanning the ablation line. Theoretically, differential pacing maneuvers (see later) may also unmask these conduction patterns.

The creation of CTI conduction block is accompanied by prolongation of the activation time required for a pacing stimulus on one side of the ablation line to propagate to the opposite side of the line (trans-isthmus interval).<sup>63</sup> In this study, before ablation the trans-isthmus intervals averaged  $100.3 \pm 21$  ms and  $98.2 \pm 25$  ms in the CW and CCW directions, respectively (pacing at 500-ms cycle length). In the presence of bidirectional isthmus block, these times increased to  $195.8 \pm 30$  ms and  $185.7 \pm 34$  ms, respectively. Bidirectional CTI block never occurred with less than a 50% prolongation in the trans-isthmus interval. An increase in the trans-isthmus interval of 50% or greater provided 100% sensitivity, 80% specificity, 89% positive predictive value, and 100% negative predictive value in confirming CTI block.

The presence of bidirectional conduction block in the CTI is strongly supported by recording widely spaced double potentials along the entire ablation line, during pacing from the low lateral right atrium or CS ostium (see Fig. 11.25).<sup>50,64</sup> When pacing from the proximal CS, intervals of less than 90 ms between EGM components anywhere on the ablation line indicates persistent conduction through a gap (Fig. 11.27, A).<sup>50</sup> When the interval between EGM components is more than 100 ms at all points along the ablation line, and maximal variation in

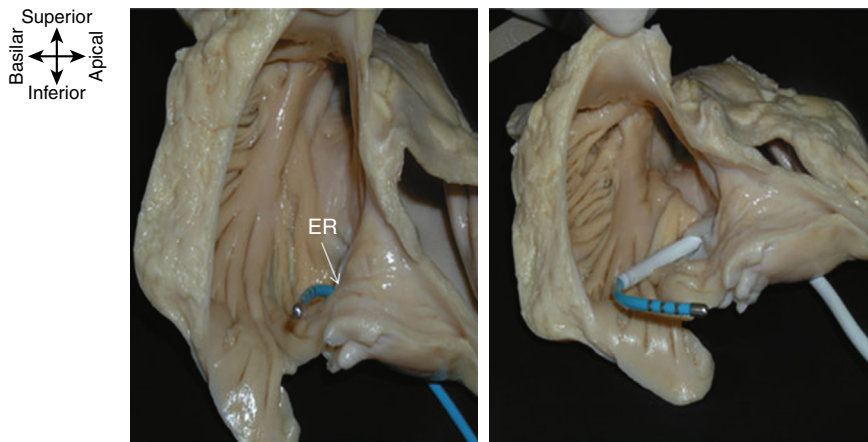


**Fig. 11.18** In this autopsy heart specimen, the catheter excursion toward the septal cavotricuspid isthmus is restricted by the Eustachian ridge (ER; *left panel*). In the *right panel*, a guiding sheath is used to direct the catheter anteriorly while curving the catheter posteriorly to reach around the Eustachian ridge. (From Asirvatham S. Correlative anatomy and electrophysiology for the interventional electrophysiologist: right atrial flutter. *J Cardiovasc Electrophysiol*. 2009; 20:113-122. With permission.)

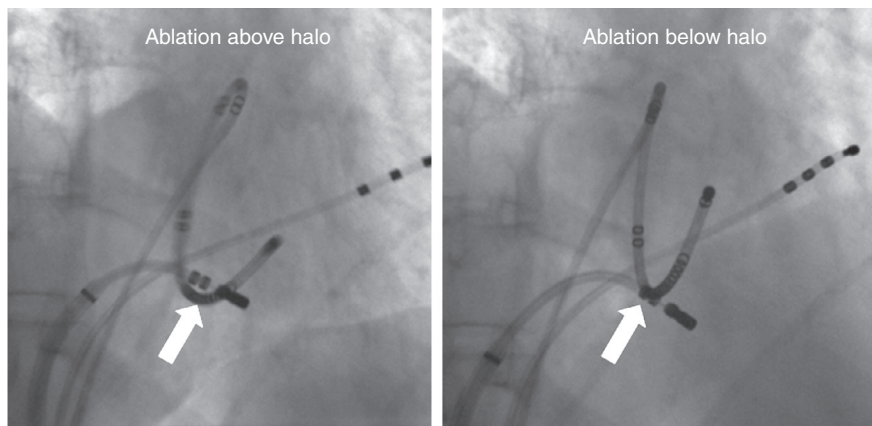


**Fig. 11.19** Shielding of the cavotricuspid (CTI) by the Halo catheter is shown in this figure. In this patient, CTI conduction block could not be achieved after repeated ablation. The ablation catheter repeatedly coursed over the Halo catheter that crosses the isthmus (arrow, *left panel*). By delivering lesions beneath the Halo catheter (arrow, *right panel*), complete CTI block was achieved.

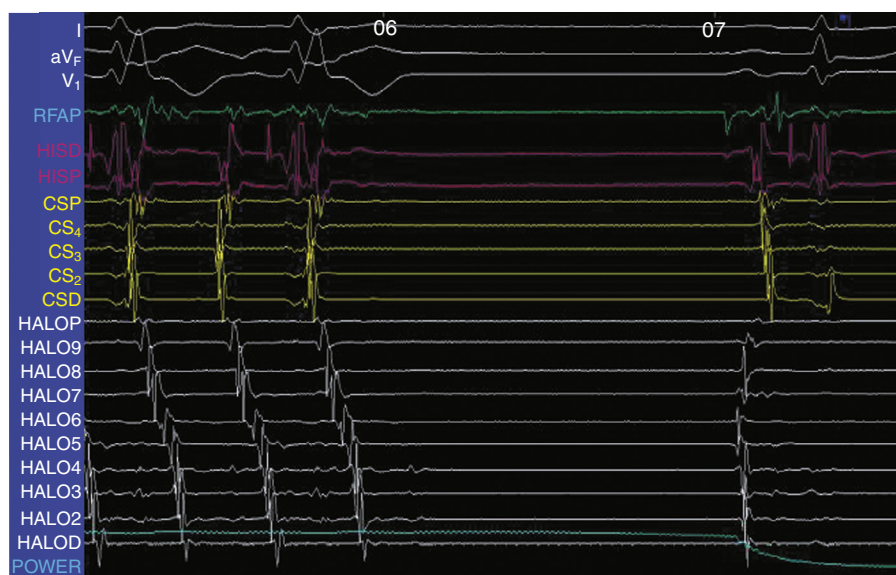


**Fig. 11.20** Termination of typical atrial flutter (AFL) during radiofrequency catheter ablation using a slow drag technique across the cavotricuspid isthmus (CTI). AFL usually terminates just as the distal ablation electrode on the mapping and ablation catheter (RFAP) approaches the inferior vena cava. Conduction fails across the CTI, as indicated by block developing between the low lateral right atrium and coronary sinus typical AFL, or between the coronary sinus and the low lateral right atrium in the reverse typical AFL (not shown). The power readout from the radiofrequency energy generator is shown in the bottom tracing. CS, Coronary sinus.

**TABLE 11.3 Methods for Confirming Cavotricuspid Isthmus Block**

Method (Reference)	Criteria for CTI Block	SENS/SPEC	PPV/NPV	Comment
Atrial activation sequence	Cranial-to-caudal activation of right atrial inferolateral free wall with PCS pacing Cranial-to-caudal activation of right atrial septum with inferior lateral right atrial pacing			Requires careful mapping adjacent to ablation line on side contralateral to pacing to exclude slow conduction through the line.
Widely split electrograms (EGM) along entire ablation line <sup>68</sup>	Interval between split atrial EGM components recorded 100%/80% along ablation line > 90 ms at all sites AND < 15 ms maximal variation among all sites during pacing from PCS	86%/100%		Interval between electrogram recordings < 90ms indicates gap in line. Recordings are from ablation catheter
Trans-isthmus interval <sup>64</sup>	CCW block: ≥50% increase in time interval between pacing stimulus from inferolateral TVA to the atrial EGM in the proximal CS CW block: >50% increase in time interval between pacing stimulus from PCS to the atrial EGM just lateral to ablation line	100%/80%	89%/100%	Minimal trans-isthmus interval associated with bidirectional CTI block approximately 140 ms
Differential pacing <sup>66</sup>	Shortening or no change in interval between pacing stimulus and latest component of split atrial EGM recorded over ablation line when pacing site moved from adjacent to line to 15 mm lateral to line When pacing close to the edge of ablation line, time to activation of contralateral side of ablation line shortens as pacing site moves away from ablation line	100%/75%	94%/100%	First pacing site should be immediately adjacent to ablation line Recording site should be immediately adjacent to ablation line
Electrogram Polarity <sup>69</sup>	Loss of negative component of unipolar atrial EGM recorded just lateral to ablation line during PCS pacing or: Reversal of EGM polarity on 2 closely spaced bipoles just lateral to the ablation line during proximal CS pacing	89%/100%	100% (PPV)	Recording must be immediately adjacent to ablation line

CCW, Counterclockwise; CS, coronary sinus; CTI, cavotricuspid isthmus; CW, clockwise; NPV, negative predictive value; PCS, proximal coronary sinus; PPV, positive predictive value; SENS, sensitivity; SPEC, specificity; TVA, tricuspid valve annulus.

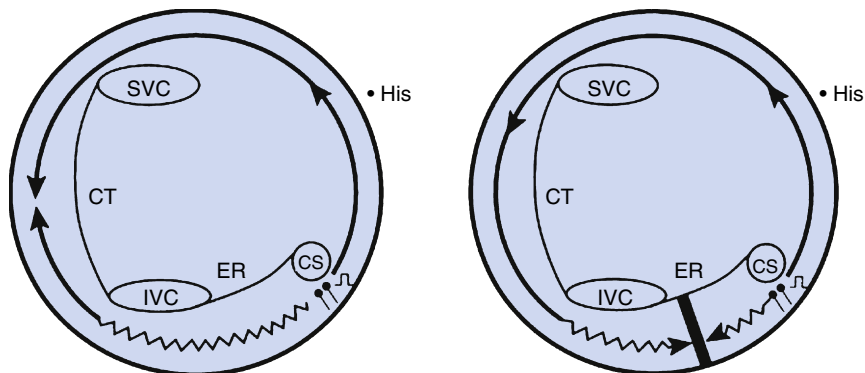


**Fig. 11.21** Schematic diagrams of the expected right atrial activation sequence during sinus rhythm from the CSos before (*left panel*) and after (*right panel*) ablation of the cavotricuspid isthmus (CTI). Before ablation, the activation pattern during CS pacing is caudal to cranial in the interatrial septum and low right atrium, with collision of the septal and right atrial wave fronts in the mid-lateral right atrium. After ablation, the activation pattern during CS pacing is still caudal to cranial in the interatrial septum, but the lateral right atrium is now activated in a strictly cranial-to-caudal pattern (i.e., counterclockwise), indicating complete medial to lateral conduction block in the CTI. *CT*, Crista terminalis; *ER*, Eustachian ridge; *His*, His bundle; *IVC*, inferior vena cava; *SVC*, superior vena cava.

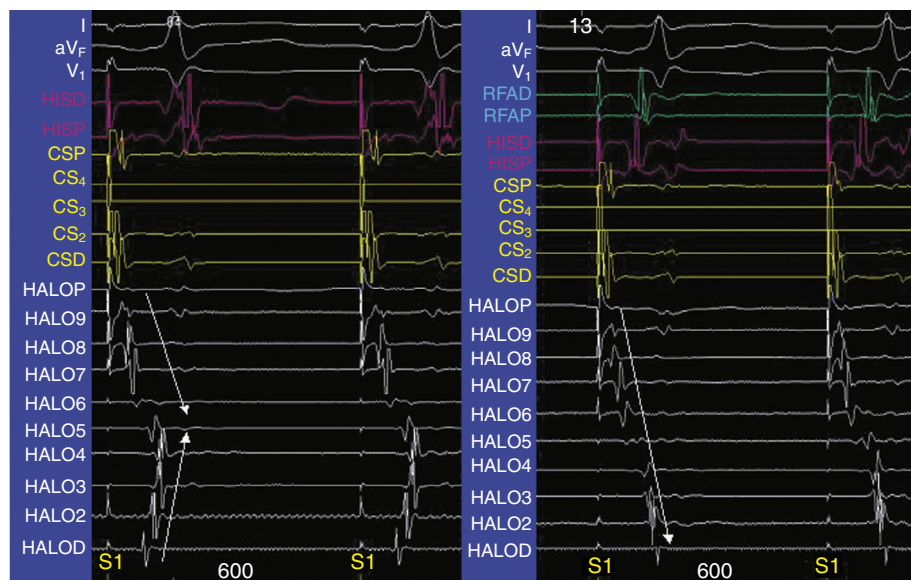


**Fig. 11.22** Surface electrocardiogram (ECG) leads and right atrial endocardial electrograms recorded during pacing in sinus rhythm from the coronary sinus (CS) ostium before (left panel) and after (right panel) ablation of the cavotricuspid isthmus (CTI). Tracings include surface ECG leads I, aVF, and V<sub>1</sub> and endocardial electrograms from the proximal coronary sinus (CSP), His bundle (HIS), tricuspid valve annulus at 1 o'clock (HALOP) to 7 o'clock (HALOD), and high right atrium (RFA). Before ablation during CS pacing, there is collision of the cranial and caudal right atrial wave fronts in the mid-lateral right atrium (HALO5). After ablation, the lateral right atrium is activated in a strictly cranial-to-caudal pattern (i.e., counterclockwise), indicating complete medial-to-lateral conduction block in the CTI.

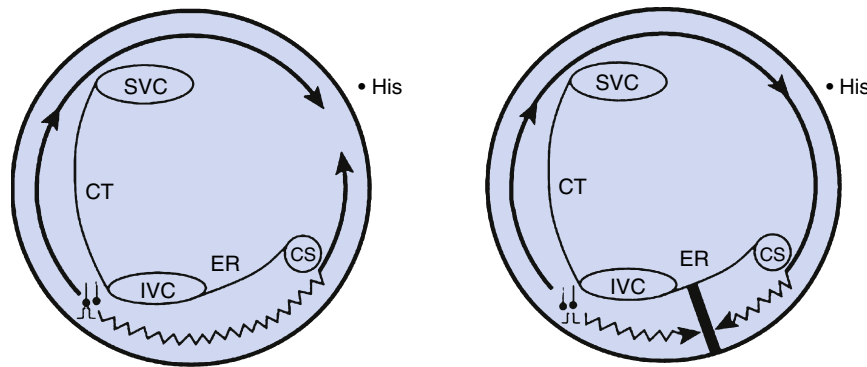


**Fig. 11.23** Schematic diagrams of the expected right atrial activation sequence during sinus rhythm from the low lateral right atrium before (left panel) and after (right panel) ablation of the cavotricuspid isthmus (CTI). Before ablation, the activation pattern during coronary sinus (CS) pacing is caudal to cranial in the right atrial free wall, with collision of the cranial and caudal wave fronts (i.e., through the CTI) in the mid-septum; there is simultaneous activation at the His bundle (HIS) and proximal coronary sinus (CSP). After ablation, the activation pattern during low lateral right atrial sinus pacing is still caudal to cranial in the right atrial free wall, but the septum is now activated in a strictly cranial-to-caudal pattern (i.e., clockwise), indicating complete counterclockwise conduction block in the CTI. CT, Crista terminalis; ER, Eustachian ridge; His, His bundle; SVC, superior vena cava.

the interval is less than 15 ms among all points, it is highly likely that bidirectional CTI is present. When mapping an incomplete ablation line, additional lesions should be given to sites with intervals less than 100 ms between EGM components and at sites in which this interval is between 90 and 110 ms if the local EGM characteristics suggest persistent conduction, including prolonged low-amplitude fractionated electrical activity in the interval between EGM components or if the second EGM component is positive in polarity. Points along the

ablation line with intervals between EGM components of more than 110 ms rarely require further ablation at that site.

Differential pacing maneuvers can be used to further demonstrate functional linking of local EGMs to a single wave front passing through the CTI in the presence of CTI conduction, or dissociation of the local EGMs in the case of conduction block.<sup>65</sup> In this technique, double potentials with an isoelectric interval (>30 ms) are recorded over the ablation line during pacing from just lateral to the line (see Fig. 11.27, B).

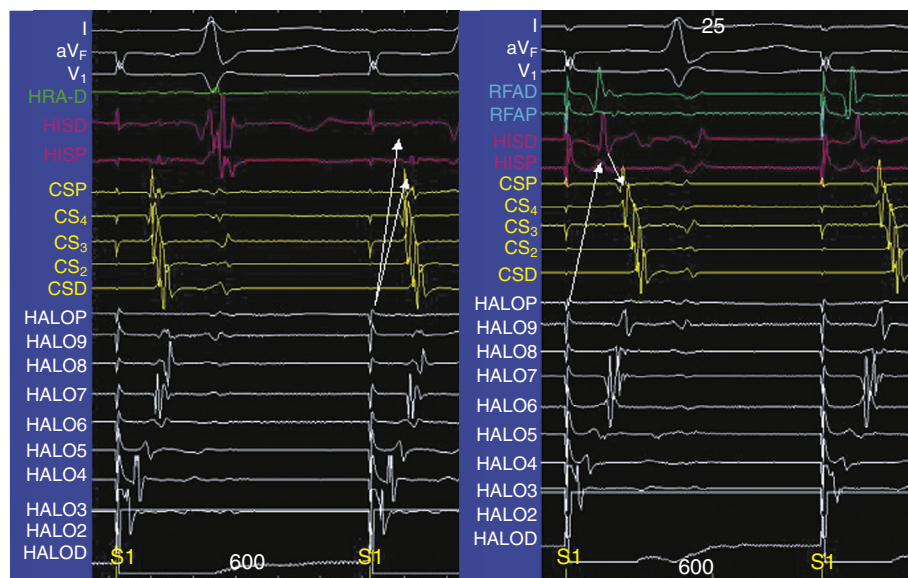


**Fig. 11.24** Surface electrocardiogram (ECG) and right atrial endocardial electrograms during pacing in sinus rhythm from the low lateral right atrium before (left panel) and after (right panel) ablation of cavitricuspid isthmus. Tracings include surface ECG leads I, aVF, and V<sub>1</sub> and endocardial electrograms from the proximal coronary sinus (CSP), His bundle (HIS), tricuspid valve annulus at 1 o'clock (HALOP) to 7 o'clock (HALOD), and high right atrium (HRA or RFA). Before ablation, during low lateral right atrial pacing, there is collision of the cranial and caudal right atrial wave fronts in the mid-septum (HIS and CSP). After ablation, the septum is activated in a strictly cranial-to-caudal pattern (i.e., clockwise), indicating complete lateral-to-medial conduction block in the CTI.

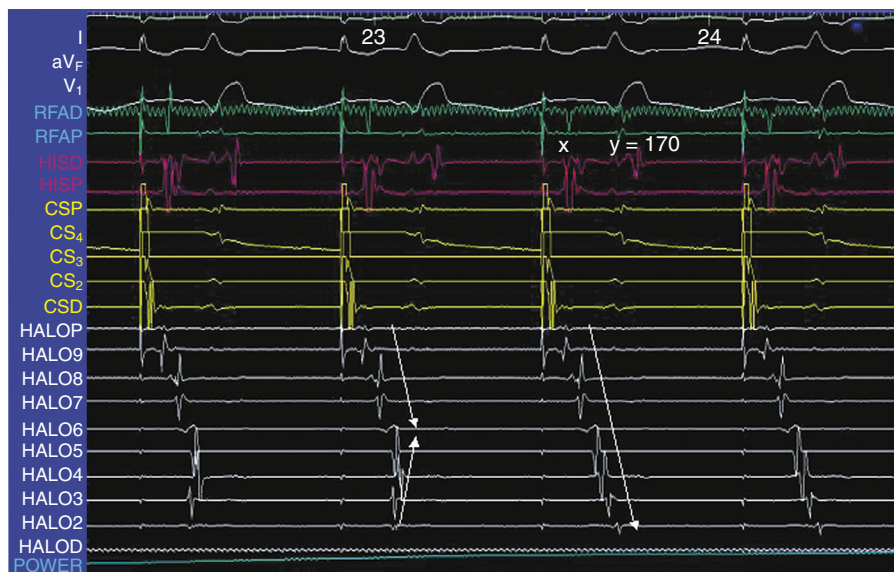


**Fig. 11.25** Surface electrocardiogram leads I, aVF, and V<sub>1</sub>, and endocardial electrograms from the coronary sinus (CS), His bundle, halo, mapping and ablation (RF), and right ventricular catheters during radiofrequency catheter ablation of the cavitricuspid isthmus (CTI), while pacing from the CS ostium. Note the change in activation of the lateral right atrium on the Halo catheter from a bidirectional to a unidirectional pattern, indicating the development of clockwise block in the CTI. This was associated with the development of widely spaced (170 ms) double potentials (x,y) on the ablation catheter in the CTI, further confirming medial-to-lateral conduction block. Halo catheter and other tracings are as described in Fig. 11.7.

The times from the stimulus to the initial and terminal components of the split EGMs are measured. The stimulus to first EGM component represents the time to activation of the ipsilateral side of the ablation line and should be 50 ms or less to demonstrate proximity. The pacing site is then moved 10 to 15 mm further lateral (away from the

ablation line) and pacing repeated. In the case of persistent CTI conduction, both components of the split EGM will be delayed or linked to the lateral to medial wave front (see Fig. 11.27 B). In the case of CTI block, however, the time to the first EGM component is delayed by  $20 \pm 9$  ms, whereas the terminal component is advanced by  $13 \pm 8$  ms,

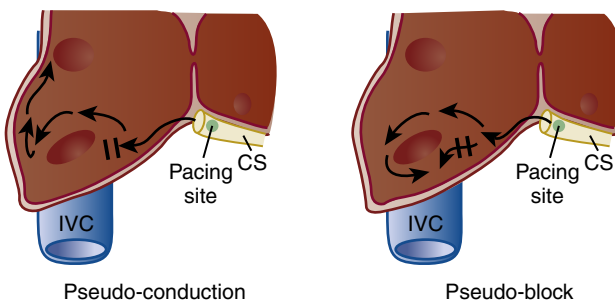


**Fig. 11.26** Patterns of conduction in the low posterior right atrium to create pseudo-conduction and pseudo-block after cavotricuspid isthmus ablation. See text for details. CS, Coronary sinus; IVC, inferior vena cava. (From Asirvatham S. Correlative anatomy and electrophysiology for the interventional electrophysiologist: right atrial flutter. *J Cardiovasc Electrophysiol*. 2009;20:113-122. With permission.)

or unchanged in timing (see Fig. 11.27 B). The delay in the terminal component indicates linking of this EGM, not to the lateral to medial wave front, but rather to that approaching the ablation line from the medial to lateral direction down the atrial septum. Using this method for detection of CTI block, the sensitivity has been shown to be 100%, specificity 75%, negative predictive value 94%, and positive predictive value 100%. For this technique to be reliable, it is important that the initial pacing site be as close as possible to the edge of the ablation line, and that the more remote pacing sites be of limited distance from the first to maintain similar propagation wave fronts. For fractionated EGMs (more than three components) on the ablation line, the first and last component should be measured. This technique may clarify the origin of fractionated potentials as caused by a conduction gap or local activation inhomogeneities. Variations on this algorithm have been introduced (Fig. 11.28 A and B).<sup>66</sup>

To expedite the assessment of bidirectional conduction block after CTI ablation and to obviate the need for multipolar electrode catheter recordings, algorithms based on reversal of EGM polarity near the ablation line and use of unipolar EGMs have also been used, with varying degrees of accuracy (Fig. 11.29).<sup>67,68</sup>

### Simplified Approach to Ablation of Cavotricuspid Isthmus-Dependent Atrial Flutter

We have developed a simplified approach for CTI ablation in patients with isthmus-dependent AFL, using only two catheters. CTI ablation can be rapidly achieved with minimal fluoroscopy time using this approach. After percutaneous insertion via the right femoral vein, a steerable decapolar catheter is positioned in the CS with the proximal electrode pair at the ostium near the medial CTI, and an ablation catheter is flexed in the low lateral right atrium with the distal pair near the lateral CTI (Fig. 11.30 A). Pacing from the proximal CS and the ablation catheter demonstrates bidirectional CTI conduction before, and block after, CTI ablation (see Fig. 11.30, B and C). Using this simplified catheter approach, medial to lateral CTI conduction block is defined by both the presence of a high to low or descending (i.e., proximal to distal) activation sequence on the ablation catheter during pacing from the proximal CS, and bidirectional conduction block by demonstrating equal conduction times (i.e., >130 ms) from medial to lateral and from lateral to medial, during pacing from the proximal CS and low lateral RA, respectively. In addition, pacing from the proximal CS with the ablation catheter positioned on

the ablation line will demonstrate widely spaced double potentials (Fig. 11.30 D).

### OUTCOMES AND COMPLICATIONS

Although early reports<sup>1-6</sup> on RFCA for CTI-dependent AFL revealed high recurrence rates (i.e., 20%–45%), increasing experience and advances in methodology and technology over time has resulted in acute and long-term success rates (defined as no recurrence of CTI-dependent AFL) as high as 85% to 95%.<sup>32-44,58</sup> For example, in a large metaanalysis comprising 10,719 patients, the long-term success rate for ablation with irrigated or large-tip RF catheters was 94% (95% confidence interval, 90%–95%) (Table 11.4).<sup>58</sup> Contributing in large degree to these improved results has been the use of large-tip or irrigated ablation catheters, and the use of bidirectional CTI conduction block as a procedural end point.<sup>32-44,58</sup> Randomized comparisons of internally cooled, externally cooled, and large-tip ablation catheters also suggest a slightly better acute and chronic success rate with the externally cooled ablation catheters.<sup>35-38,44</sup>

Despite the excellent acute and long-term results for AFL ablation, the development of atrial fibrillation after CTI ablation alone occurs at a high rate in this population (up to 67% over 5 years), especially if there is a history of atrial fibrillation or underlying heart disease before CTI ablation.<sup>58,69,70</sup> By metaanalysis, the occurrence rate of atrial fibrillation at 1 to 2 years follow-up was 23% in those without a history of atrial fibrillation before ablation, and 53% in those with a prior history of atrial fibrillation.<sup>58</sup> At 5 years' follow-up, the occurrence rate of atrial fibrillation was similar (i.e., 60%) regardless of atrial fibrillation history before ablation.<sup>58</sup>

Ablation of CTI-dependent AFL is relatively safe, with complication rates of 2.5% to 3.5%.<sup>56</sup> Most complications are caused by peripheral vascular injury (0.4% of patients), but serious complications can rarely occur, including heart block (0.2% of patients), pericardial effusion and tamponade (0.1% of patients), myocardial infarction from right coronary artery injury, and thromboembolic events, including pulmonary embolism and stroke.<sup>58</sup>

Although conversion of AFL to sinus rhythm is less likely than atrial fibrillation to cause thromboembolic complications (e.g., stroke), there is still a significant risk, and oral anticoagulation before ablation must be considered in patients who have persistent CTI-dependent AFL.<sup>71</sup> This may be particularly important in those patients with depressed left ventricular function, mitral valve disease, or left atrial enlargement with spontaneous contrast (i.e., smoke) on echocardiography. As an alternative to oral anticoagulation, transesophageal echocardiography may be used to rule out left atrial clot immediately before CTI ablation, but subsequent to conversion of AFL to sinus rhythm during CTI ablation, oral anticoagulation must be continued for at least 30 days because of potential atrial stunning, similar to that seen following conversion of atrial fibrillation.<sup>71</sup>

### TROUBLESHOOTING THE DIFFICULT CASE

Despite the high ablation success rates reported in recent studies, difficult AFL ablation cases may still be occasionally encountered. In these cases, several measures can be used to increase the likelihood of successful ablation (Fig. 11.31; Table 11.5). First, it is critically important to ensure that the mechanism of the spontaneous or induced AFL is CTI dependent. If multi-electrode catheter mapping with pacing entrainment is not sufficient to confirm CTI dependence

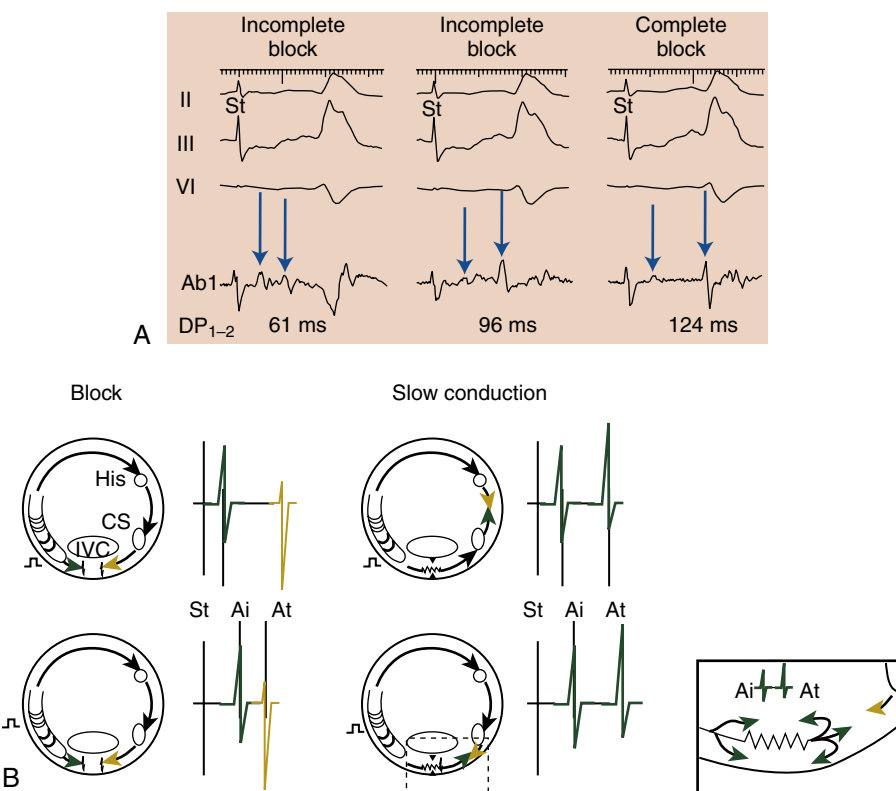


**Fig. 11.27** Methods of determining bidirectional cavotricuspid isthmus (CTI) conduction block after ablation. A, Recordings during coronary sinus (CS) pacing before (left and middle) and after (right) complete CTI block are shown. Displayed are leads II, III and V1, electrograms recorded by the ablation catheter (Abl). The arrows in the electrograms recorded by the Abl point to the components of the double potentials (DPs). The Abl was positioned at exactly the same site in all three panels. *Left*, After several applications of radiofrequency energy along the ablation line, the interval separating the two components of DPs (DP<sub>1-2</sub>) is 61 ms, and there is incomplete block. *Middle*, After an additional application of radiofrequency energy, the DP<sub>1-2</sub> interval increases to 96 ms, but isthmus block is still incomplete. *Right*, After a final application of radiofrequency energy, the DP<sub>1-2</sub> interval lengthens to 124 ms, and now there is complete block. Note that when the DP<sub>1-2</sub> interval was 96 ms, the segment separating the two components of the DP was not isoelectric, providing further evidence that there was a persistent gap in the ablation line. On the transition to complete block, the segment with the DP became isoelectric. St, Stimulus artifact. (From Tada H, Oral H, Sticherling C, et al. Double potentials along the ablation line as a guide to radiofrequency ablation of typical atrial flutter. *J Am Cardiol Coll*. 2000;138:750-755. With permission.). B, Schematic representation of activation principles on which assessment is based. Right atrium and selected key structures [IVC, His bundle, coronary sinus ostium (Cs)] are shown in a cartoon format. A quadripolar catheter is shown and activation is pictured during distal bipole stimulation (*top row*) and proximal bipole stimulation (*bottom row*). Shown are activation patterns during complete isthmus block (*left*) and during persistent but slow isthmus conduction through a gap in the ablation line (*right*). During complete isthmus block, double potentials separated by an isoelectric interval are recorded on the ablation line as a result of two opposing fronts: a descending front (shown in blue) and another that detours around isthmus (in brown) give rise to double potentials Ai (initial potential) and At (terminal potential) (blue and brown, respectively). On changing to a proximal stimulation site, descending wave front (in blue) has to travel a longer distance to reach line of block, whereas detouring wave front (in brown) has a shorter distance to travel; as a result, Ai (blue potential) is delayed, and At (brown potential) is advanced. During persistent isthmus conduction through a gap in the ablation line, double potentials are recorded as a result of delayed activation of downstream isthmus by the same blue front, and therefore both resulting potentials (Ai and At) are shown in blue (inset, far right). When stimulation is performed from a proximal site, activation pattern does not change, but descending wave front (in blue) has a longer distance to travel to reach isthmus line; as a result, both blue potentials (Ai and At) are delayed. St, stimulus artifact. (From Shah D, Haissaguerre M, Takahashi A, et al. Differential pacing for distinguishing block from persistent conduction through an ablation line. *Circulation*. 2000;102:1517-1522. With permission.)

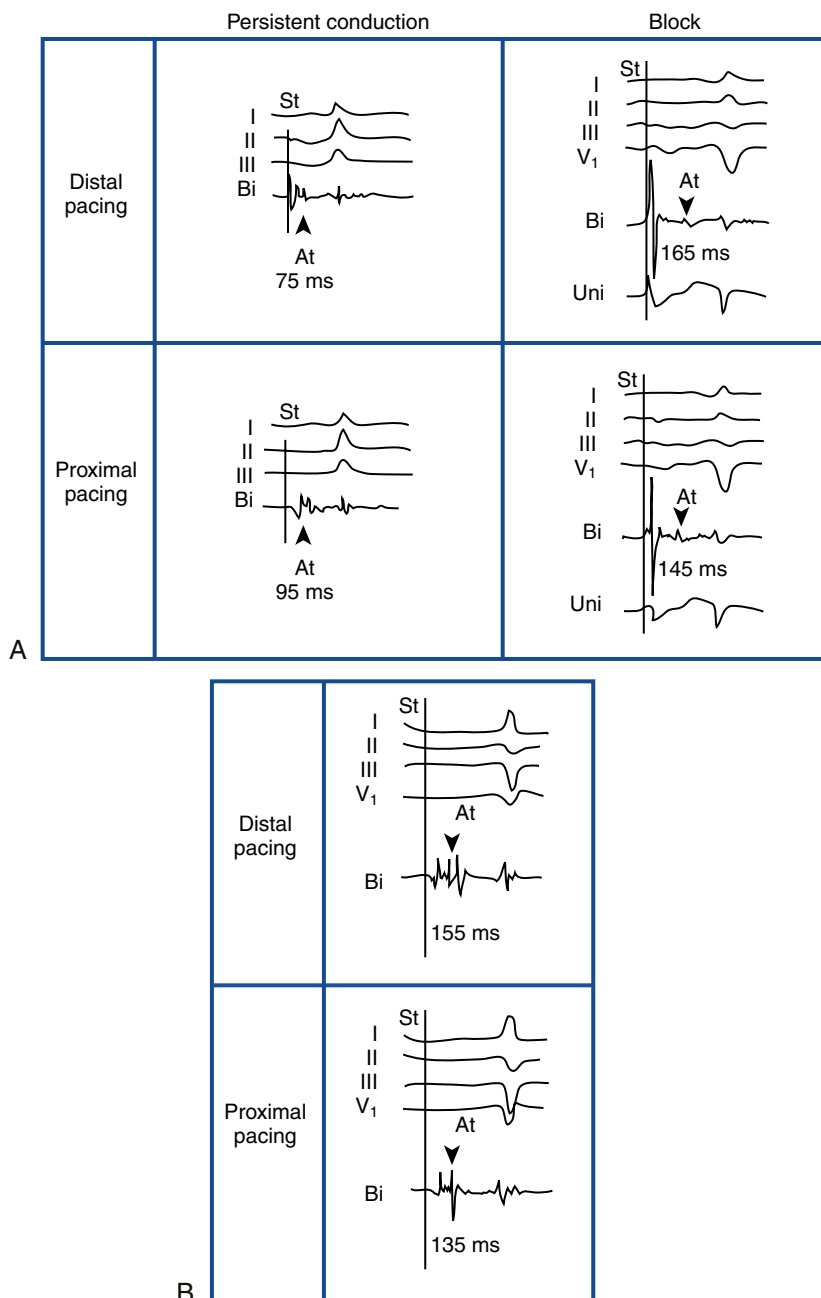


**Fig. 11.28** Differential pacing to assess for cavotricuspid isthmus (CTI) conduction block. A, Representative examples of assessment in different patients. *Top left*, double potentials with a stimulus to second potential timing of 75 ms are recorded from isthmus during pacing from distal bipolar. The stimulus to first potential timing is 20 ms. As shown in the *bottom left panel*, during pacing from the proximal bipolar, both potentials are delayed by 20 ms so that second potential is now activated at 95 ms. This response indicates persistent conduction. Further ablation was performed in the CTI to produce complete conduction block. Surface electrocardiogram (ECG) leads shown are I, II, and III. *Right*, Double potentials with a large first potential and a small second potential are recorded. During distal bipolar pacing, as shown in the *top row*, first potential is activated at 15 ms, and second potential is activated at 165 ms after stimulus. During pacing from proximal bipolar, *below*, first potential is delayed by 20 ms and second potential is advanced by 20 ms (145 ms). Note that morphology of both potentials remains unchanged, in bipolar as well as in unipolar electrograms (*lowest trace*). This response indicates complete isthmus block. Surface ECGs include leads I, II, III, and V<sub>1</sub>. *Bi*, bipolar electrogram; *Uni*, unipolar electrogram. B, Bystander slow conduction and complete block in the presence of a triple potential. A complex triple potential was recorded along the ablation line after documentation of complete CTI conduction block. Compared with the top tracing, which was recorded during stimulation from distal bipolar, as shown on bottom right, which was recorded during proximal bipolar stimulation, the first and second components are delayed identically without a change in their morphology by 25 ms, whereas the third and terminal component, which is also morphologically unchanged, is advanced by 20 ms (155–135 ms). This response indicates that complete conduction block exists between second and third components and that first two components are directly linked to each other by a single front of slow or circuitous conduction. (From Shah D, Haissaguerre M, Takahashi A, et al. Differential pacing for distinguishing block from persistent conduction through an ablation line. *Circulation*. 2000;102:1517-1522. With permission.)

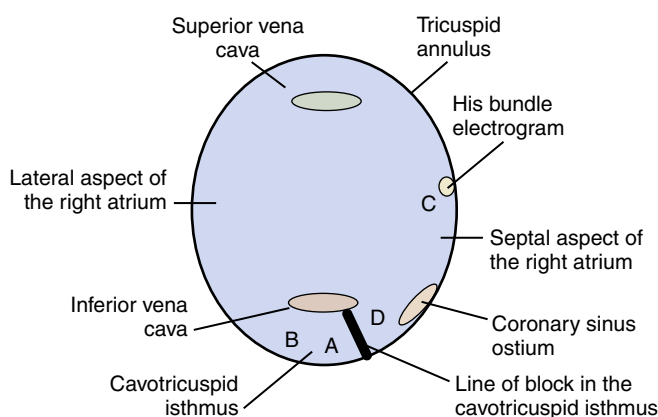
**Methods:** Pacing at sites (A, B, C and D) on both sides of ablation line and record bipolar EGM activation times at points A, B, C and D pre- and post ablation.

**Measure:** Conduction times among sites A, B, C, and D

**Definition of complete isthmus block:**

Conduction times A D > B D and D A > C A after ablation

**Reference:** Chen. *Circulation* 1999; 100:2507-2513

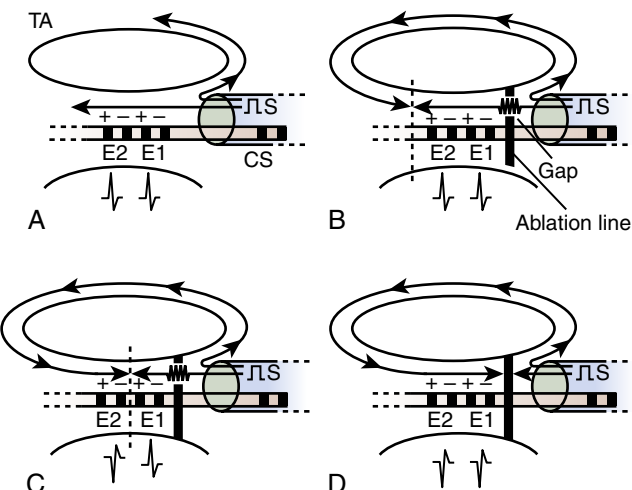


**Methods:** Pacing PCS and record 2 bipolar EGM (E1 and E2, 2 mm spacing each) 2 mm apart just lateral to ablation line

**Measure:** Polarity of E1 and E2 during PCS pacing pre- and post ablation

**Definition of isthmus block:** Transition of EGM polarity from positive to negative at both E1 and E2

**Reference:** Tada. *JCE* 2001, 12:393-399



**Methods:** Unipolar EGM recording during PCS pacing pre- and post ablation

**Measure:** Unipolar EGM polarity immediately lateral to ablation line

**Definition of isthmus complete block:**

Loss of negative components and development of R or Rs pattern in unipolar EGM

**Reference:** Villacastin. *Circulation* 2000; 102: 3080-3085

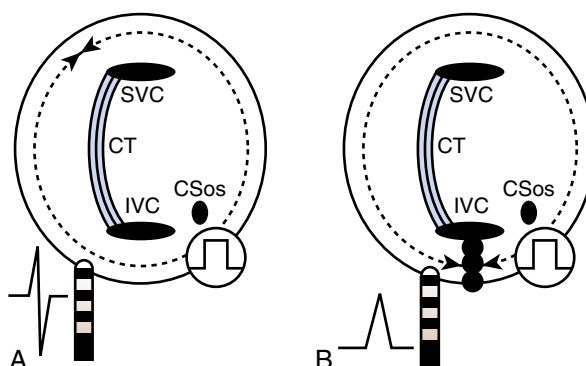


**Fig. 11.29** Additional methods of defining cavotricuspid isthmus (CTI) conduction block. *Top*, Use of conduction times measured at line of block. In the presence of CTI block, moving the pacing site away from the ablation line shortens the distance to the contralateral side of the line and shortens the conduction time. In the presence of conduction through the line, the distance is prolonged, and the conduction times lengthen. *Middle*, Bipolar electrograms (EGMs) close to the edge of the ablation line reveal the direction of activation of each bipole. In the presence of CTI conduction block, both bipolar EGM pairs are activated by a wave front propagating toward the ablation line. In the presence of CTI conduction block, one or both bipoles are activated by a wave front propagating away from the ablation line. *Bottom*, In the presence of CTI conduction block, a unipolar EGM recorded immediately adjacent to the ablation line records only an activation wave front approaching the electrode and no activation past the edge of the line. In this case, the EGM is entirely positive. CS, coronary sinus; CSos, coronary sinus ostium; CT, computed tomography; IVC, inferior vena cava; PCS, proximal coronary sinus; SVC, superior vena cava. (*Top*, from Chen J, de Chilou C, Basiouny T, et al. Cavotricuspid isthmus mapping to assess bidirectional block during common atrial flutter radiofrequency ablation. *Circulation*. 1999;100:2507-2513; *middle*, from Tada H, Oral H, Sticherling C, et al. EGM polarity and cavotricuspid isthmus block during ablation of typical atrial flutter. *J Cardiovasc Electrophysiol*. 2001;12:393-399, *bottom*, from Villacastin J, Almendral J, Arenal A, et al. Usefulness of unipolar electrograms to detect isthmus block after radiofrequency ablation of typical atrial flutter. *Circulation*, 2000;102:3080-3085. With permission.)

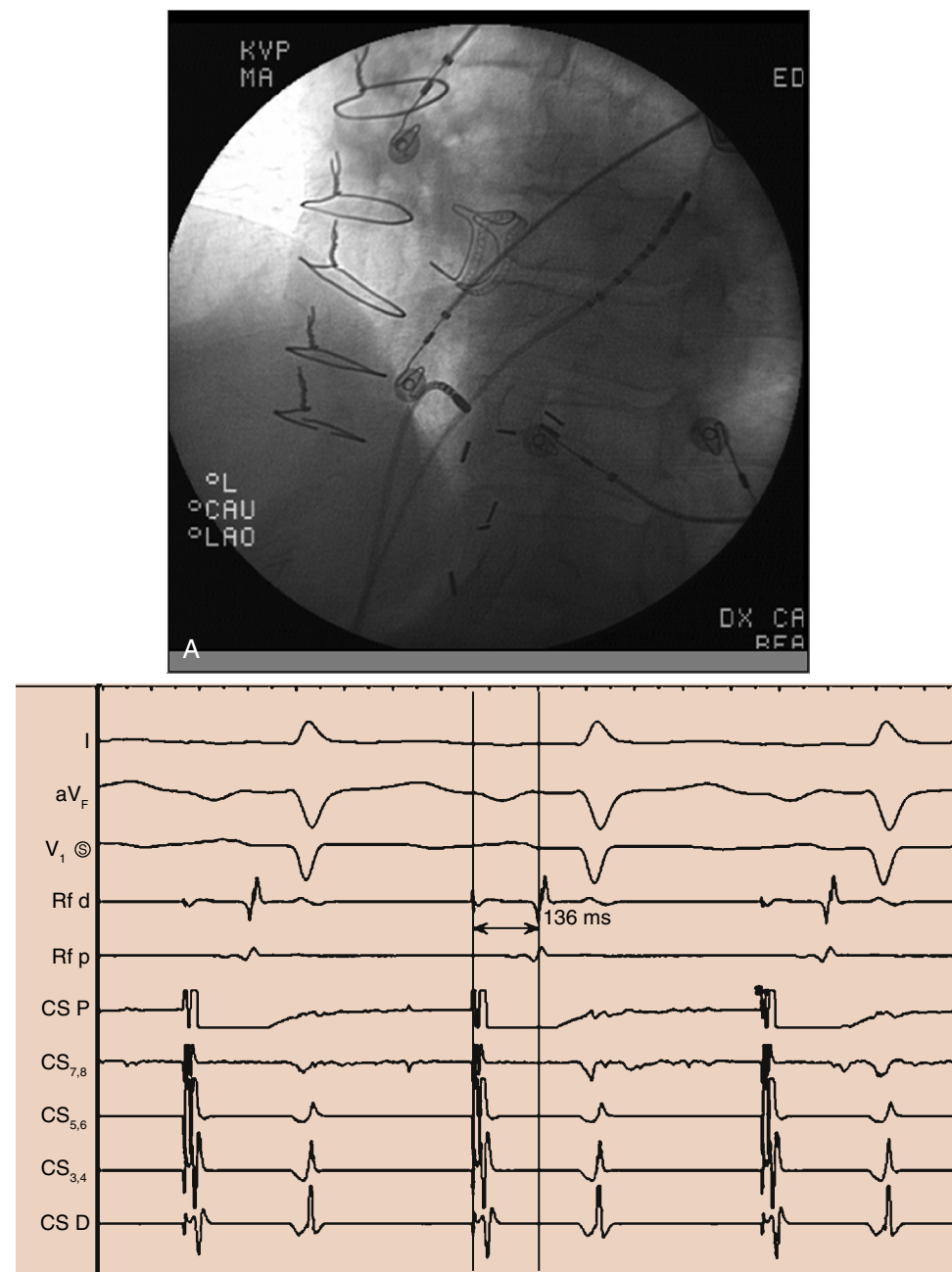


**Fig. 11.30** A, Left anterior oblique fluoroscopic projection showing the positions of the coronary sinus (CS) and ablation catheter after cavotricuspid isthmus (CTI) ablation to demonstrate conduction block. The proximal CS catheter electrode is positioned near the CS ostium, and the ablation catheter is positioned at the lateral CTI. B, Surface electrocardiogram (ECG) and endocardial electrogram recordings during pacing from the proximal CS demonstrating a proximal to distal (high to low) activation sequence on the ablation catheter with a conduction time of 136 ms confirming medial to lateral CTI conduction block. *I*, *aVF*, *V*<sub>1</sub>, surface ECG leads; *Rf d&p*, distal and proximal ablation catheter electrograms; *CSd-p*, distal to proximal CS electrograms. C, Surface ECG and endocardial electrogram recordings during pacing from the ablation catheter at the low lateral right atrium demonstrating a conduction time to the proximal CS of 138 ms, similar to the medial to lateral conduction time, confirming lateral to medial CTI conduction block. Abbreviations same as in 16B. D, Surface ECG and endocardial electrogram recordings during pacing from the proximal CS demonstrating widely spaced (130 ms) double potentials (X and Y) at the ablation line, confirming medial to lateral conduction block. Abbreviations same as in previous figures. (From Sawhney NS, Wayne Whitwam W, Feld GK. Mapping of human atrial flutter and its variants. In: Shenasa M, Hindricks G, Borggreve M, Briethardt G, eds. *Cardiac Mapping*, 4th ed. Hoboken NJ: Wiley-Blackwell; 2012:191-212, with permission.)

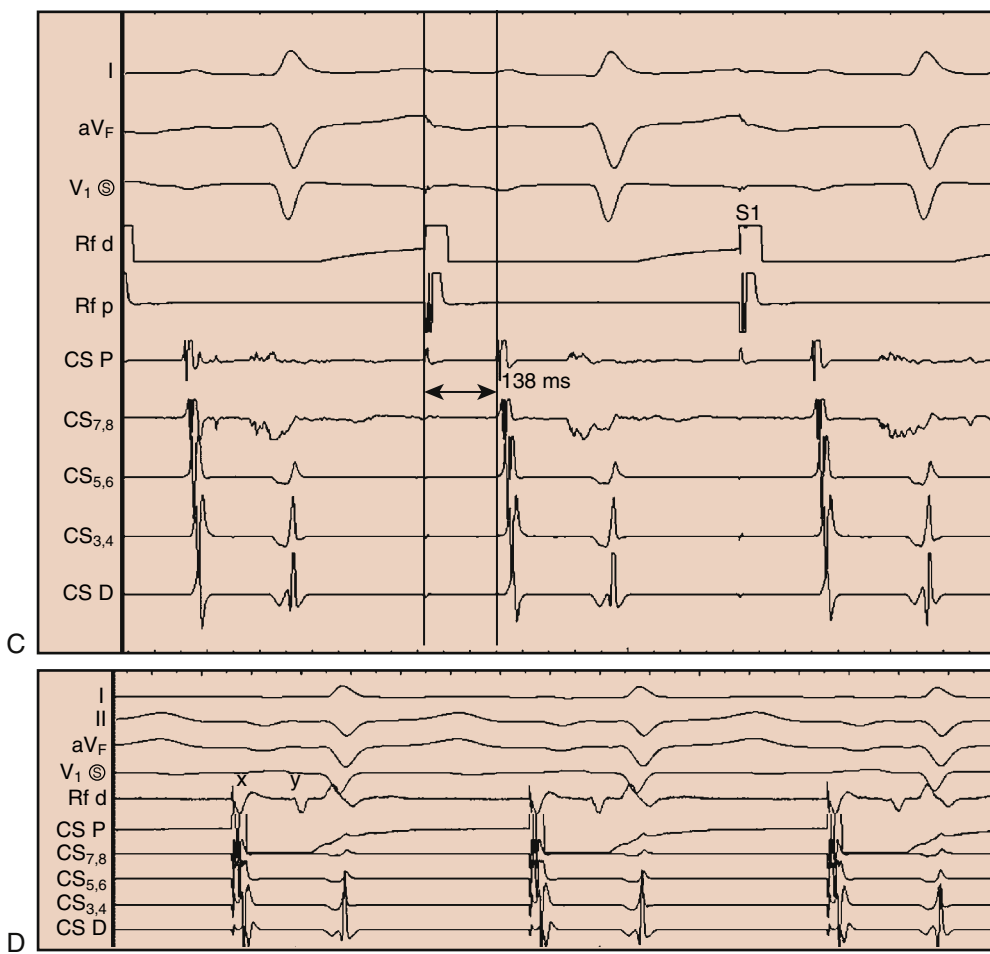


Fig. 11.30, cont'd.

TABLE 11.4 Metaanalysis of Ablation Outcomes Based on Catheter Technology

Catheter Type	Acute Success Number of Studies/Patients	Acute Success % (95% CI)	AFL Recurrence Number of Studies/Patients	AFL Recurrence % (95% CI)
4–6 mm RF	16/512	86 (78, 92)	17/529	18 (15, 21)
8–10 mm or Irrigated RF	49/3098	94 (91, 95)	49/3052	7 (5, 8)

AFL, Atrial flutter; RF, radiofrequency.

Data from Perez FJ, Schubert CM, Parvez B, et al. Long-term outcomes after catheter ablation of cav o-tricuspid isthmus dependent atrial flutter: a meta-analysis. *Circ Arrhythm Electrophysiol*. 2009;2:393–401.

of the AFL, then 3-dimensional computerized activation mapping may be helpful for confirmation and to rule out other mechanisms.

Once the CTI dependence of the AFL has been confirmed, if initial ablation attempts are unsuccessful, it is essential to ensure that the ablation catheter has reached the extreme borders of the CTI isthmus, including the TVA and Eustachian ridge or IVC. This may require the use of large-curve catheters or the use of preformed guiding sheaths, such as the Schwartz Left 1, Schwartz Right 0 (SL1, SR0), or ramp sheaths, to ensure catheter contact across the entire CTI. Careful mapping of the CTI with the mapping or ablation catheter may also help identify a gap in the ablation line (using criteria noted earlier), which when ablated may terminate AFL and produce bidirectional CTI conduction block (see Fig. 11.11). Persistent CTI conduction after initial failed ablation may sometimes be identified by 3-dimensional computerized activation mapping, if use of

standard multi-electrode catheters has been unsuccessful. Isthmus pouches are present in many patients and may not be ablated without specific catheter maneuvers. The presence of a pouch may be visualized by angiography, ICE, or electroanatomic mapping. The visualization of complex isthmus anatomy early in the case may facilitate a more rapid and successful conclusion.<sup>72</sup>

We recommend that ablation be performed in the 6 o'clock position on the TVA initially. If this is unsuccessful and CTI block cannot be achieved even after elimination of apparent gaps in the line, a new ablation line should be created more laterally, at the 7 or 8 o'clock position on the tricuspid annulus. Large right atrial trabeculae may enter the lateral CTI tangentially and require extensive ablation to achieve bidirectional conduction block. If this is also ineffective, an ablation line may then be created more medially, at the 5 o'clock position, but care must be taken in this position to monitor AV conduction because the risk

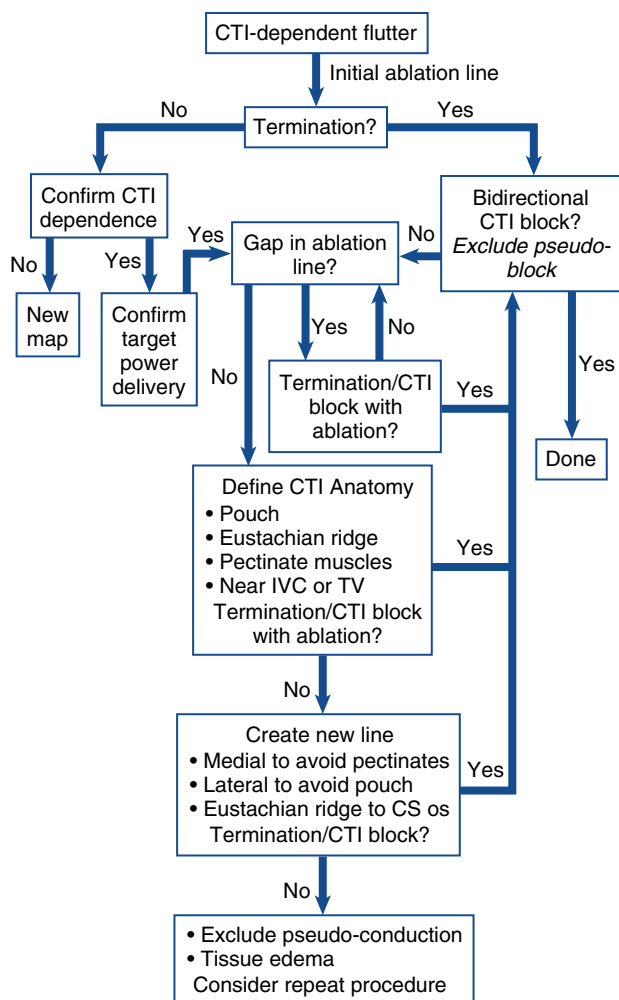


**Fig. 11.31** Schematic diagram for sequence of events during cavotricuspid isthmus (CTI) ablation. CS, Coronary sinus; IVC, inferior vena cava; TV, tricuspid valve.

**TABLE 11.5 Troubleshooting Difficult Cases**

Problem	Cause	Solution
Lack of AFL termination	Non-CTI dependent AFL as original rhythm or change circuit with ablation Incomplete ablation line because of poor tissue contact, low energy delivery, difficult anatomy Partial-isthmus reentry	Repeat activation, entrainment mapping, map ablation line for gaps, use steerable or preformed sheath, use large tip or irrigated ablation catheter, angiography, ICE or EA mapping for pouch, large Eustachian ridge, pectinate muscles, confirm target energy delivery, deliver new line more lateral or medial, ablate under Halo™ if crosses isthmus Ablate between IVC and CS os
Unable to achieve lasting bidirectional CTI	Incomplete ablation line because of poor tissue contact, low energy delivery, difficult anatomy Pseudoconduction posterior to IVC Partial-isthmus reentry Tissue edema after extensive ablation	Map ablation line for gaps, use steerable or preformed sheath, use large tip or irrigated ablation, angiography, ICE, EA mapping for pouch, large Eustachian ridge, pectinate muscles, deliver new line more lateral or medial, ablate under Halo if crosses isthmus, confirm target energy delivery, detailed mapping with electrodes spanning ablation line, possibly differential pacing maneuvers Ablate between Eustachian ridge and CS os Create new ablation line, increase power delivery, schedule second procedure after tissue recovery
Low RF energy delivery	Low blood flow caused by ablation in pouch, Eustachian ridge, or between pectinate muscles	Use irrigated catheter or cryoablation, create new line avoiding unfavorable anatomy
Poor catheter reach, stability, or unable to navigate to target sites	Enlarged right atrium/IVC, large Eustachian ridge (limits septal excursion), large pectinate muscles	Use preformed or steerable sheath to stabilize catheter, use longer reach and/or stiffer catheter, angle sheath anteriorly and catheter curvature posteriorly to reach around Eustachian ridge, ablation from superior vena cava approach

for AV block is increased. It is important to give sufficient RF energy at each site. Marked tissue edema may occur after the initial energy delivery, thereby insulating the tissue from further ablation. If new lines fail, voltage-guided ablation of the CTI can be undertaken. Typically, an ablation temperature of 60°C is recommended for CTI ablation with solid nonirrigated ablation catheter, or a power of 40 to 45 W for irrigated catheters, but occasionally successful CTI ablation requires a temperature as high as 70°C for nonirrigated or power as high as 50 W for irrigated catheters, respectively. If standard ablation electrodes of 4 or 5 mm are used initially and ablation fails, the use of either a large-tip (8–10 mm) ablation catheter with a high-power generator or an irrigated-tip catheter is recommended. We prefer large-tip (8–10 mm) or cooled-tip catheters as the first-line approach for CTI ablation because they have been shown to have greater efficacy than standard catheters in most studies, or at least to produce CTI conduction block with fewer energy applications and shorter procedure times. The use of temperatures exceeding 70°C, with standard or large-tip ablation catheters, or energy exceeding 50 W with irrigated-tip catheters, in an attempt to improve success rates is not recommended because of the increased risk for steam pops, which can cause cardiac rupture.

If CTI block cannot be achieved, the presence of pseudoconduction should be excluded. After extended ablation, tissue edema may make further energy delivery futile, and a second procedure may be necessary.

**TABLE 11.5 Troubleshooting Difficult Cases—cont'd**

<b>Problem</b>	<b>Cause</b>	<b>Solution</b>
Failure to attenuate/ eliminate local electrograms	Low energy delivery Poor tissue contact Large pectinate muscles in CTI	See earlier See earlier Increase energy delivery, use sheaths, create new line medially
Painful ablation	Electrical/thermal stimulation Deep sedation of cardiac nerves	Use deep sedation
Changing atrial activation pattern during AFL	Figure-of-eight reentry in right atrium, intermittent crista terminalis Breakthrough, intermittent lower loop reentry	Remapping for sustained new activation patterns, use noncontact mapping, reassess after creating CTI block

AFL, Atrial flutter; AV, atrioventricular; CS, coronary sinus; CTI, cavitricuspid isthmus; EA, electroanatomical; ICE, intracardiac echocardiography; IVC, inferior vena cava; os, ostium; RF, radiofrequency energy.

## REFERENCES

1. Saoudi N, Cosio F, Waldo A, et al. Classification of atrial flutter and regular atrial tachycardia according to electrophysiologic mechanism and anatomic bases: a statement from a joint expert group from the Working Group of Arrhythmias of the European Society of Cardiology and the North American Society of Pacing and Electrophysiology. *J Cardiovasc Electrophysiol.* 2001;12:852–866.
2. Feld GK, Fleck RP, Chen PS, et al. Radiofrequency catheter ablation for the treatment of human type 1 atrial flutter: identification of a critical zone in the re-entrant circuit by endocardial mapping techniques. *Circulation.* 1992;86:1233–1240.
3. Cosio FG, Lopez-Gil M, Goicoechea A, et al. Radiofrequency ablation of the inferior vena cava-tricuspid valve isthmus in common atrial flutter. *Am J Cardiol.* 1993;71:705–709.
4. Lesh MD, Van Hare GF, Epstein LM, et al. Radiofrequency catheter ablation of atrial arrhythmias: results and mechanisms. *Circulation.* 1994;89:1074–1089.
5. Cosio FG, Goicoechea A, Lopez-Gil M, et al. Atrial endocardial mapping in the rare form of atrial flutter. *Am J Cardiol.* 1990;66:715–720.
6. Tai CT, Chen SA, Chiang CE, et al. Electrophysiologic characteristics and radiofrequency catheter ablation in patients with clockwise atrial flutter. *J Cardiovasc Electrophysiol.* 1997;8:24–34.
7. Olshansky B, Okumura K, Gess PG, et al. Demonstration of an area of slow conduction in human atrial flutter. *J Am Coll Cardiol.* 1990;16:1639–1648.
8. Feld GK, Mollerius M, Birgersdotter-Green U, et al. Conduction velocity in the tricuspid valve-inferior vena cava isthmus is slower in patients with a history of atrial flutter compared to those without atrial flutter. *J Cardiovasc Electrophysiol.* 1997;8:1338–1348.
9. Kinder C, Kall J, Kopp D, et al. Conduction properties of the inferior vena cava-tricuspid annular isthmus in patients with typical atrial flutter. *J Cardiovasc Electrophysiol.* 1997;8:727–737.
10. Da Costa A, Mourot S, Romeyer-Bouchard C, et al. Anatomic and electrophysiological differences between chronic and paroxysmal forms of common atrial flutter and comparison with controls. *Pacing Clin Electrophysiol.* 2004;27:1202–1211.
11. Feld GK, Shahandeh-Rad F. Mechanism of double potentials recorded during sustained atrial flutter in the canine right atrial crush-injury model. *Circulation.* 1992;86:628–641.
12. Olglin JE, Kalman JM, Fitzpatrick AP, et al. Role of right atrial endocardial structures as barriers to conduction during human type 1 atrial flutter: activation and entrainment mapping guided by intracardiac echocardiography. *Circulation.* 1995;92:1839–1848.
13. Olglin JE, Kalman JM, Lesh MD. Conduction barriers in human atrial flutter: correlation of electrophysiology and anatomy. *J Cardiovasc Electrophysiol.* 1996;7:1112–1126.
14. Kalman JM, Olglin JE, Saxon LA, et al. Activation and entrainment mapping defines the tricuspid annulus as the anterior barrier in typical atrial flutter. *Circulation.* 1996;94:398–406.
15. Cabrera JA, Sanchez-Quintana D, Farre G, et al. The inferior right atrial isthmus: further architectural insights for current and coming ablation technologies. *J Cardiovasc Electrophysiol.* 2005;16:402–408.
16. Cabrera JA, Ho SY, Sanchez-Quintana D. How anatomy can guide ablation in isthmic atrial flutter. *Europace.* 2009;11:4–6.
17. Lim K-T, Murray C, Liu H, Weerasooriya R. Pre-ablation magnetic resonance imaging of the cavotricuspid isthmus. *Europace.* 2007;9:149–153.
18. DaCosta A, Romeyer-Bouchard C, Dauphinot V, et al. Cavotricuspid isthmus angiography predicts atrial flutter ablation efficacy in 281 patients randomized between 8 mm- and externally irrigated-tip catheter. *Eur Heart J.* 2006;27:1833–1840.
19. Chang SL, Tai CL, Lin YJ, et al. The electroanatomic characteristics of the cavotricuspid isthmus: implications for the ablation of atrial flutter. *J Cardiovasc Electrophysiol.* 2007;18:18–22.
20. Gami A, Edwards W, Lachman N, et al. Electrophysiological anatomy of typical atrial flutter: the posterior boundary and causes for difficulty with ablation. *J Cardiovasc Electrophysiol.* 2010;21:144–149.
21. Tai CT, Huang JL, Lee PC, et al. High-resolution mapping around the crista terminalis during typical atrial flutter: new insights into mechanisms. *J Cardiovasc Electrophysiol.* 2004;15:406–414.
22. Spach MS, Miller III WT, Dolber PC, et al. The functional role of structural complexities in the propagation of depolarization in the atrium of the dog: cardiac conduction disturbances due to discontinuities of effective axial resistivity. *Circ Res.* 1982;50:175–191.
23. Spach MS, Dolber PS, Heidlage JF. Influence of the passive anisotropic properties on directional differences in propagation following modification of sodium conductance in human atrial muscle: a model of reentry based on anisotropic discontinuous propagation. *Circ Res.* 1998;62:811–832.
24. Olglin JE, Kalman JM, Saxon LA, et al. Mechanisms of initiation of atrial flutter in humans: site of unidirectional block and direction of rotation. *J Am Coll Cardiol.* 1997;29:376–384.
25. Yang Y, Cheng J, Bochoeyer A, et al. Atypical right atrial flutter patterns. *Circulation.* 2001;103:3092–3098.
26. Bochoeyer A, Yang Y, Cheng J, et al. Surface electrocardiographic characteristics of right and left atrial flutter. *Circulation.* 2003;108:60–66.
27. Yang Y, Varma N, Badhwar N, et al. Prospective observations in the clinical and electrophysiological characteristics of intra-isthmus reentry. *J Cardiovasc Electrophysiol.* 2010;21:1099–1106.
28. Yang Y, Varma N, Keung EC, Scheinman MM. Reentry within the cavotricuspid isthmus: an isthmus dependent circuit. *Pacing Clin Electrophysiol.* 2005;28:808–818.
29. Oshikawa N, Watanabe I, Masaki R, et al. Relationship between polarity of the flutter wave in the surface ECG and endocardial atrial activation sequence in patients with typical counterclockwise and clockwise atrial flutter. *J Interv Card Electrophysiol.* 2002;7:215–223.
30. Okumura K, Plumb VJ, Page PL, et al. Atrial activation sequence during atrial flutter in the canine pericarditis model and its effects on the polarity of the flutter wave in the electrocardiogram. *J Am Coll Cardiol.* 1991;17:509–518.
31. Chugh A, Latchamsetty R, Oral H, et al. Characteristics of cavotricuspid isthmus-dependent atrial flutter after left atrial ablation of atrial fibrillation. *Circulation.* 2006;113:609–615.
32. Fischer B, Haissaguerre M, Garrigue S, et al. Radiofrequency catheter ablation of atrial flutter in 80 patients. *J Am Coll Cardiol.* 1995;25:1365–1372.
33. Kirkorian G, Moncada E, Chevalier P, et al. Radiofrequency ablation of atrial flutter: efficacy of an anatomically guided approach. *Circulation.* 1994;90:2804–2814.
34. Chen SA, Chiang CE, Wu TJ, et al. Radiofrequency catheter ablation of common atrial flutter: comparison of electrophysiologically guided focal ablation technique and linear ablation technique. *J Am Coll Cardiol.* 1996;27:860–868.
35. Jais P, Haissaguerre M, Shah DC, et al. Successful irrigated-tip catheter ablation of atrial flutter resistant to conventional radiofrequency ablation. *Circulation.* 1998;98:835–838.
36. Atiga WL, Worley SJ, Hummel J, et al. Prospective randomized comparison of cooled radiofrequency versus standard radiofrequency energy for ablation of typical atrial flutter. *Pacing Clin Electrophysiol.* 2002;25:1172–1178.
37. Scavee C, Jais P, Hsu LF, et al. Prospective randomized comparison of irrigated-tip and large-tip catheter ablation of cavotricuspid isthmus-dependent atrial flutter. *Eur Heart J.* 2004;25:963–969.
38. Calkins H. Catheter ablation of atrial flutter: do outcomes of catheter ablation with “large-tip” versus “cooled-tip” catheters really differ? *J Cardiovasc Electrophysiol.* 2004;15:1131–1132.
39. Matsuo S, Yamane T, Tokuda M, et al. Prospective randomized comparison of a steerable versus a non-steerable sheath for typical atrial flutter ablation. *Europace.* 2010;12:402–409.
40. DaCosta A, Romeyer-Bouchard C, Jamon Y, et al. Radiofrequency catheter selection based on cavotricuspid angiography compared with a control group with an externally irrigated catheter: a randomized pilot study. *J Cardiovasc Electrophysiol.* 2009;20:492–498.
41. Feld GK. Radiofrequency ablation of atrial flutter using large-tip electrode catheters. *J Cardiovasc Electrophysiol.* 2004;15:S18–S23.
42. Feld GK, Wharton M, Plumb V. EPT-1000 XP Cardiac Ablation System Investigators. Radiofrequency catheter ablation of type 1 atrial flutter using large-tip 8- or 10-mm electrode catheters and a high-output radiofrequency energy generator: results of a multicenter safety and efficacy study. *J Am Coll Cardiol.* 2004;43:1466–1472.

43. Kumar S, Morton JB, Lee G, et al. High Incidence of low catheter-tissue contact force at the cavotricuspid isthmus during catheter ablation of atrial flutter: implications for achieving isthmus block. *J Cardiovasc Electrophysiol.* 2015;26:826–831.
44. Venier S, Andrade JG, Khairy P, et al. Contact-force-guided vs. contact-force-blinded catheter ablation of typical atrial flutter: a prospective study. *Europace.* 2017;19:1043–1048.
45. Hindricks G, Willems S, Kautzner J, et al. Effect of electroanatomically guided versus conventional catheter ablation of typical atrial flutter on the fluoroscopic time and resource use: a prospective randomized multicenter study. *J Cardiovasc Electrophysiol.* 2009;20:734–740.
46. Nakagawa H, Lazzara R, Khastgir T, et al. Role of the tricuspid annulus and the Eustachian valve/ridge on atrial flutter: relevance to catheter ablation of the septal isthmus and a new technique for rapid identification of ablation success. *Circulation.* 1996;94:407–424.
47. Nakagawa H, Imai S, Schleinkofer M, et al. Linear ablation from tricuspid annulus to Eustachian valve and ridge is adequate for patients with atrial flutter: extending ablation line to the inferior vena cava is not necessary. *J Am Coll Cardiol.* 1997;29:199A.
48. Gula L, Redferns DP, Veenhuyzen GD, et al. Reduction in atrial flutter ablation time by targeting maximal voltage: results of a prospective randomized clinical trial. *J Cardiovasc Electrophysiol.* 2009;20:1108–1112.
49. Bauerfeind T, Kardos A, Foldesi C, et al. Assessment of the maximal voltage-guided technique for cavotricuspid isthmus ablation during ongoing atrial flutter. *J Interv Card Electrophysiol.* 2007;19:195–199.
50. Tada H, Oral H, Sticherling C, et al. Double potentials along the ablation line as a guide to radiofrequency ablation of typical atrial flutter. *J Am Coll Cardiol.* 2001;38:750–755.
51. Chan JY, Fung JW, Yu CM, Feld GK. Preliminary results with percutaneous transcatheater microwave: optimizing the detection of bidirectional block across the flutter isthmus for patients with typical isthmus-dependent atrial flutter. *Am J Cardiol.* 2003;91:559–564.
52. Asirvatham SJ. Correlative anatomy and electrophysiology for the interventional electrophysiologist: right atrial flutter. *J Cardiovasc Electrophysiol.* 2009;20:113–122.
53. Stovicek P, Fikar M, Wichterl D. Temporal pattern of conduction recurrence during radiofrequency ablation for typical atrial flutter. *J Cardiovasc Electrophysiol.* 2006;17:628–631.
54. Schwartzman D, Callans D, Gottlieb CD, et al. Conduction block in the inferior caval-tricuspid valve isthmus: association with outcome of radiofrequency ablation of type 1 atrial flutter. *J Am Coll Cardiol.* 1996;28:1519–1531.
55. Nabar A, Rodriguez L, Timmermans C, et al. Isoproterenol infusion to evaluate resumption of conduction after atrial isthmus ablation in Type I atrial flutter. *Circulation.* 1999;99:3286–3291.
56. Poty H, Saoudi N, Aziz AA, et al. Radiofrequency catheter ablation of type 1 atrial flutter: prediction of late success by electrophysiologic criteria. *Circulation.* 1995;92:1389–1392.
57. Mangat I, Tschoop Jr DD, Yang Y, et al. Optimizing the detection of bidirectional block across the flutter isthmus for patients with typical isthmus-dependent atrial flutter. *Am J Cardiol.* 2003;91:559–564.
58. Perez FJ, Schubert CM, Parvez B, et al. Long-term outcomes after catheter ablation of cavo-tricuspid isthmus dependent atrial flutter: a meta-analysis. *Circ Arrhythmia Electrophysiol.* 2009;2:393–401.
59. Arenal A, Almendral J, Alday JM, et al. Rate-dependent conduction block of the crista terminalis in patients with typical atrial flutter: influence on evaluation of cavotricuspid isthmus conduction block. *Circulation.* 1999;99:2771–2778.
60. Liu TY, Tai CT, Huang BH, et al. Functional characterization of the crista terminalis in patients with atrial flutter: implications for radiofrequency ablation. *J Am Coll Cardiol.* 2004;43:1639–1645.
61. Anselme F, Savoure A, Ouali S, et al. Transcristal conduction during isthmus ablation of typical atrial flutter: influence on success criteria. *J Cardiovasc Electrophysiol.* 2004;15:184–189.
62. Scaglione M, Riccardi R, Calo L, et al. Typical atrial flutter ablation: conduction across the posterior region of the inferior vena cava may mimic unidirectional isthmus block. *J Cardiovasc Electrophysiol.* 2000;11:387–395.
63. Oral H, Sticherling C, Tada H, et al. Role of transisthmus intervals in predicting bidirectional block after ablation of typical atrial flutter. *J Cardiovasc Electrophysiol.* 2001;12:169–174.
64. Tai CT, Haque A, Lin YK, et al. Double potential interval and transisthmus conduction time for prediction of cavotricuspid isthmus block after ablation of typical atrial flutter. *J Interv Card Electrophysiol.* 2002;7:77–82.
65. Shah D, Haissaguerre M, Takahashi A, et al. Differential pacing for distinguishing block from persistent conduction through an ablation line. *Circulation.* 2000;102:1517–1522.
66. Chen J, de Chillou C, Basiouny T, et al. Cavotricuspid isthmus mapping to assess bidirectional block during common atrial flutter radiofrequency ablation. *Circulation.* 1999;100:2507–2513.
67. Tada H, Oral H, Sticherling C, et al. Electrogram polarity and cavotricuspid isthmus block during ablation of typical atrial flutter. *J Cardiovasc Electrophysiol.* 2001;12:393–399.
68. Villacastin J, Almendral J, Arenal A, et al. Usefulness of unipolar electrograms to detect isthmus block after radiofrequency ablation of typical atrial flutter. *Circulation.* 2000;102:3080–3085.
69. Gilligan DM, Zakaib JS, Fuller I, et al. Long-term outcome of patients after successful radiofrequency ablation for typical atrial flutter. *Pacing Clin Electrophysiol.* 2003;26:53–58.
70. Tai CT, Chen SA, Chiang CE, et al. Long-term outcome of radiofrequency catheter ablation for typical atrial flutter: risk prediction of recurrent arrhythmias. *J Cardiovasc Electrophysiol.* 1998;9:115–121.
71. Gronefeld GC, Wegener F, Israel CW, et al. Thromboembolic risk of patients referred for radiofrequency catheter ablation of typical atrial flutter without prior appropriate anticoagulation therapy. *Pacing Clin Electrophysiol.* 2003;26:323–327.
72. Da Costa A, Romeyer-Bouchard C, Jamon Y, et al. Radiofrequency catheter selection based on cavotricuspid angiography compared with a control group with an externally cooled-tip catheter: a randomized pilot study. *J Cardiovasc Electrophysiol.* 2009;20:492–498.